

Supporting Information for

A study of acridine and acridinium-substituted bis(terpyridine)zinc(II) and ruthenium(II) complexes as photosensitizers for O₂ (¹Δ_g) generation

Jens Eberhard,^{*a} Katrin Peuntinger,^b Susann Rath,^a Beate Neumann,^c Hans-Georg Stammmer,^c Dirk M. Guldi,^b and Jochen Mattay^{*a}

^a Organische Chemie I, Fakultät für Chemie, Universität Bielefeld, Universitätsstr. 25, 33501 Bielefeld, Germany. Phone: +49 521 106 2072; E-mail: mattay@uni-bielefeld.de, jens.eberhard@uni-bielefeld.de

^b Physikalische Chemie I, Department of Chemistry and Pharmacy and Interdisciplinary Center for Molecular Materials, Friedrich-Alexander-Universität Erlangen-Nürnberg, Egerlandstr. 3, 91058 Erlangen, Germany.

^c Abteilung für Röntgenstrukturanalyse, Fakultät für Chemie, Universität Bielefeld, Universitätsstr. 25, 33501 Bielefeld, Germany.

Contents

1 Experimental	S3
1.1 Materials and methods	S3
1.1.1 Instrumentation for routine characterization	S3
1.1.2 Software	S3
1.1.3 Solvents and Reagents	S4
2 Additional X-ray data representations	S5
3 Additional spectroscopic data	S6
4 Photocatalytic experiments	S7
4.1 Exemplary UV/Vis spectra for the photooxidation of DHN	S7
4.2 Limonene and 2-methylnaphthalene irradiation experiments	S13
4.2.1 Photooxidation of limonene	S13
4.2.2 Attempted photooxidation of 2-methylnaphthalene	S19
4.3 Actinometry	S20
4.3.1 Transmission of NaNO ₂ filter solution	S22
5 Analytical data	S23
5.1 NMR data of the zinc(II) complexes	S23
5.1.1 [Zn(ATT) ₂][PF ₆] ₂ (1)	S23

5.1.2 [Zn(MeATT) ₂][PF ₆] ₄ (2)	S29
5.2 IR data	S36
5.3 MS data	S37
6 Computational methods	S38
6.1 Comparison of X-ray data and calculated geometry	S38
6.2 Comparison of IR frequency data	S38
6.3 HOMO and LUMO analysis	S39
6.4 Spin density plots	S41
6.5 TD-DFT results	S41
6.6 Geometries for [Zn(ATT) ₂] ²⁺ (1)	S43
6.6.1 Optimized S ₀ geometry (MeCN)	S43
6.6.2 Optimized T ₁ geometry (MeCN)	S45
6.7 Geometries for [Zn(MeATT) ₂] ⁴⁺ (2)	S48
6.7.1 Optimized S ₀ geometry (MeCN)	S48
6.7.2 Optimized T ₁ geometry (MeCN)	S50

1 Experimental

1.1 Materials and methods

1.1.1 Instrumentation for routine characterization

Melting points (mp, uncorrected) were measured with a Büchi B-540 electrothermal melting point apparatus.

NMR spectra were recorded on a Bruker DRX 500 (^1H operating at 500.13 MHz, ^{13}C at 125.76 MHz), Bruker Avance AV 500 (^1H operating at 500.01 MHz, ^{13}C at 125.0 MHz), Bruker Avance AV 600 (^1H operating at 600.13 MHz, ^{13}C at 150.9 MHz), or on a Bruker Avance AV 300 (^1H operating at 300.13 MHz, ^{13}C at 75.468 MHz, ^{19}F operating at 282.40 MHz). The residual proton, ^1H , or ^{13}C resonances^[1] of the > 99 % deuterated solvents were used for internal reference of all spectra acquired (CDCl_3 : ^1H 7.260 ppm, ^{13}C 77.16 ppm, $\text{DMSO}-d_6$: ^1H 2.500 ppm, ^{13}C 39.52 ppm, $\text{MeCN}-d_3$: ^1H 1.940 ppm, ^{13}C 1.32 ppm, Nitromethane- d_3 : ^1H 4.330 ppm, ^{13}C 63.80 ppm). J values are given in Hz. Assignments are based on 2D spectra (COSY, HMQC; see below) and comparison to the corresponding ruthenium(II) complexes.^[2]

Standalone EI mass spectra were recorded with a Micromass VG Autospec X double focusing, triple sector mass spectrometer (EBE geometry) equipped with a standard EI source. Electrospray ionization (ESI) mass spectrometry were done on a Bruker Daltonics Esquire 3000. High resolution mass spectrometry (HRMS) were measured with a Bruker Daltonics Apex III (7 T) fourier transform ion cyclotron resonance (FT-ICR) instrument with either nano-ESI inlet or ionization by a MALDI-source. Routine MALDI spectra were recorded on a Applied Biosystems Voyager MALDI-ToF equipped with a nitrogen laser (3 Hz repetition rate) at 20 kV and 105 ns delay time. 2-[(2-E)-3-(4-*tert*-butylphenyl)-2-methyl-2-propenylidene]malononitrile (DCTB, in-house synthesis) (in neat CH_2Cl_2) or 2,5-dihydroxybenzoic acid (DHB, 99 %, Sigma-Aldrich) (in $\text{CHCl}_3/\text{MeOH}$ 1:1 (v/v)) were used as matrices.

GC/MS spectra were measured with a Shimadzu GC17A/QP5050A gas chromatograph/-mass spectrometry couple equipped with a standard EI source (70 eV). A standard HP-5MS column (25 m × 0.2 mm fused-silica with 0.33 µm cross-linked 5 % phenyl, 95 % methyl siloxane layer) was used for separation with the following temperature program employed: 4 min 75 °C isotherm than ramp up to 280 °C with 10 °C min⁻¹ and finally 6.5 min isotherm at this temperature. Injection port temperature: 250 °C. Total gas flow (He): 31.5 mL min⁻¹, column: 0.7 mL min⁻¹, split ratio: 40. Linear velocity: 33.8 cm s⁻¹.

IR spectra were recorded on a Thermo Scientific Nicolet 380 FT-IR with a Smart Orbit Diamond ATR cell and resolution set to 2.00 cm⁻¹. Data processing was done by using the OMNIC Software v7.3. Only strong and very strong bands of the finger-print region are given in the main text. See spectroscopic section (IR sec. 5.2) for the full spectra.

Elemental analysis was carried out by the in-house microanalytical service of Bielefeld University on a HEKAttech EuroEA CHN analyzer.

1.1.2 Software

Bond lengths, angles *etc.* of X-ray and calculated structures were examined using Mercury v3.1 (RC 5). The spin density and HOMO-LUMO isocontour plots and RMSD

examination of the calculated structures (Fig S. 41) were made by use of Jmol *v*13.3.5.^[3]. Calculated frequency and TD-DFT data were exported by use of Swizard *v*4.7 with a FWHM for IR bands of 15 cm⁻¹.^[4] Orbital energy plots and fragment analysis were made with Chem3D *v*3.3.^[5] All other data plots were made with Origin *v*8.5G.

1.1.3 Solvents and Reagents

Solvents were dried according to standard procedures or purchased in suitable purity (e.g. HPLC grade) from well-known suppliers (VWR International, Fisher Scientific, Carl Roth), and used immediately after opening (especially in case of acetonitrile (MeCN)).

The following commercially available starting materials were used as received: (−)-carveol (> 97 % mixture of *cis* and *trans* isomer, VWR), (+)-limonene (> 98 % sum of enantiomers, Fluka), methylene blue chloride dihydrat ([MB][Cl] × 2 H₂O, microscopy grade, Merck). 2-methylnaphthalene (anal. std., Sigma), [Ru(bpy)₃][Cl]₂ × 6 H₂O (98 %, Acros), and, zinc trifluoromethanesulfonate (Zn(OTf)₂, 98 %, Alfa Aesar).

1,5-Dihydroxynaphthalene (DHN 98 %, TCI) was recrystallized from EtOH/H₂O (1:1 v/v, ≈ 50 mL g⁻¹) by additional use of activated charcoal. The hot mixture was filtered by gravity in a precooled round bottom flask (ice/water bath) and was let cool under a gentle stream of argon. By this procedure fine colorless needle were obtained from an almost colorless motherliquid. Recovery was about 64 %.

2 Additional X-ray data representations

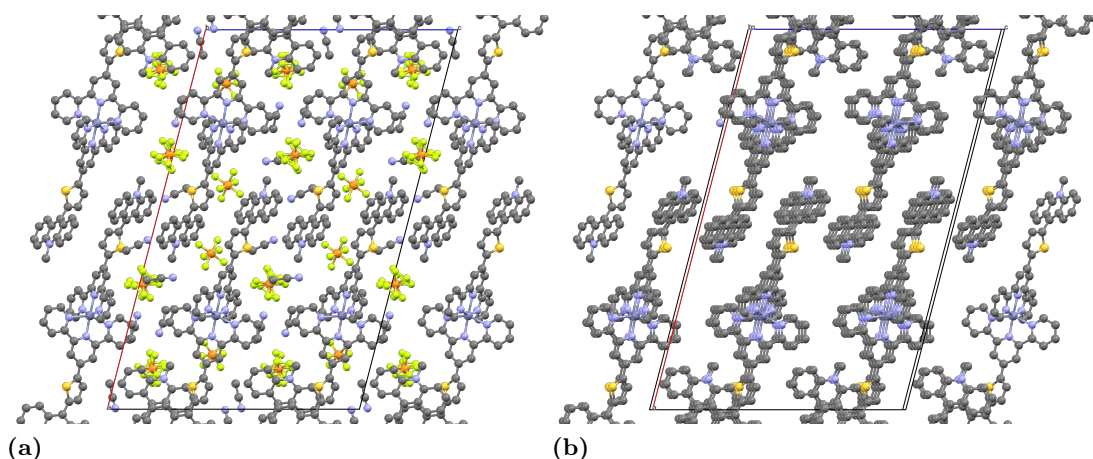


Fig. S 1 View on the packing of $[\text{Zn}(\text{MeATT})_2][\text{PF}_6]_4 \times 5 \text{ MeCN}$ along the b -axis. Hydrogen atoms are omitted for clarity (a). In (b) MeCN solvent molecules and PF_6^- counterions are additionally hidden and the view is changed to b -axis+ 2° to emphasize the layering of the complex ion in the crystal.

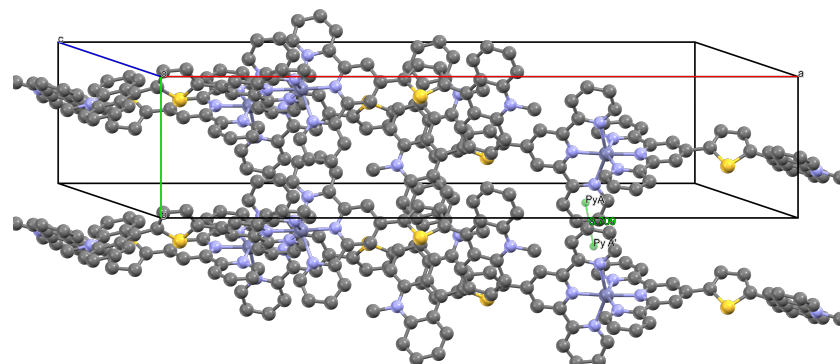


Fig. S 2 View on the (fractional occupied for clarity) unit cell of $[\text{Zn}(\text{MeATT})_2][\text{PF}_6]_4 \times 5 \text{ MeCN}$ along the inverse c -axis- 5° to emphasize the interaction (dashed green line) of the outer pyridyl-rings (Py^A) of the terpyridine fragment.

3 Additional spectroscopic data

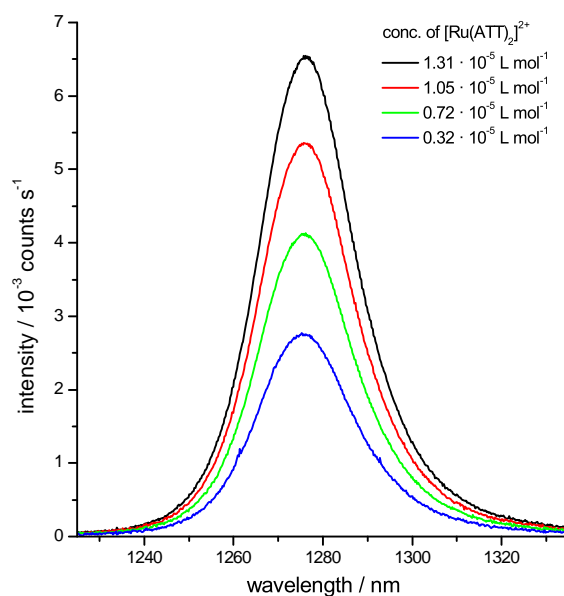


Fig. S 3 NIR emission of singlet oxygen at 1275 nm induced by irradiation of $[\text{Ru}(\text{ATT})_2]^{2+}$ (4) at $\lambda_{\text{ex.}}$ 504 nm with different sensitizer concentrations used (calc. from OD) in oxygen-saturated MeCN solution at rt.

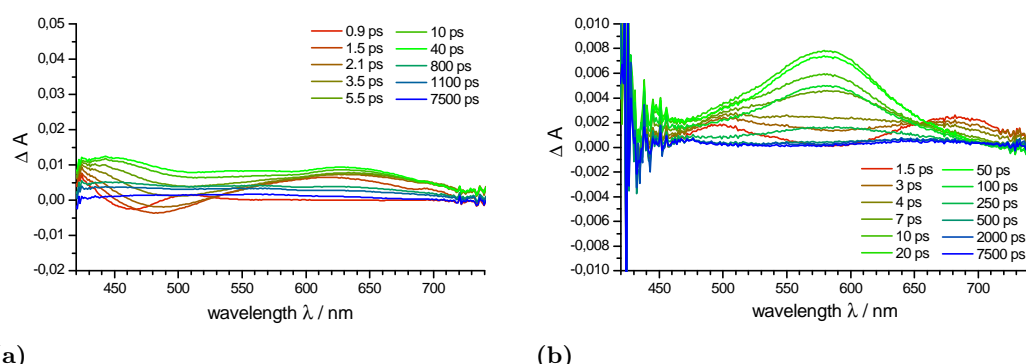


Fig. S 4 Differential absorption spectra upon fs flash photolysis (387 nm, $200 \text{ nJ pulse}^{-1}$) of the ATT ligand (a) and $[\text{Zn}(\text{MeATT})_2]^{4+}$ (2) (b) in deaerated MeCN with several time delays between 0.9 and 7500 ps.

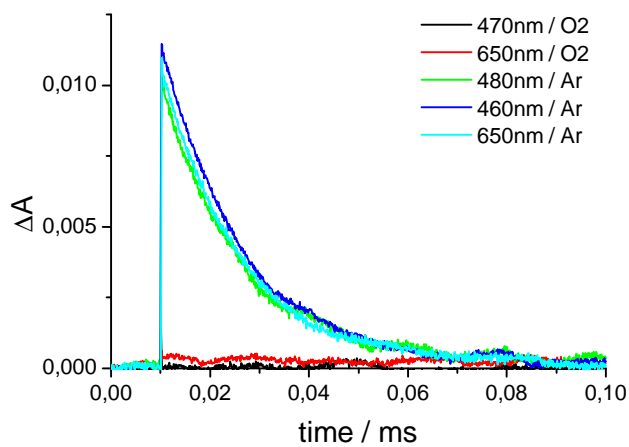


Fig. S 5 Transient absorption decay of $[Zn(ATT)_2]^{2+}$ (1) monitored at different wavelengths in argon and oxygen-saturated MeCN solution, respectively.

4 Photocatalytic experiments

4.1 Exemplary UV/Vis spectra for the photooxidation of DHN

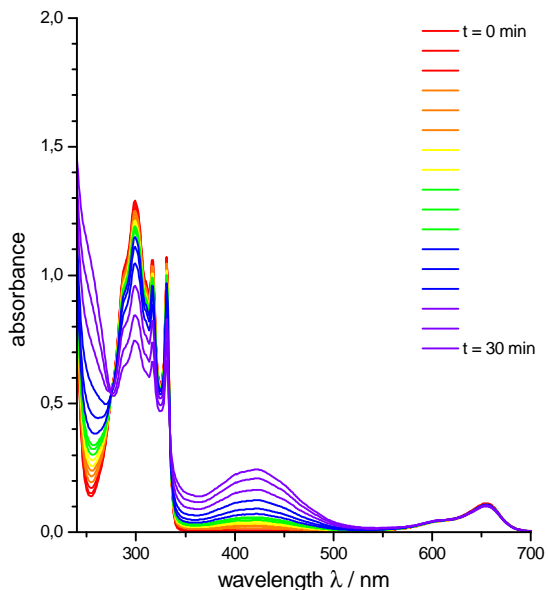


Fig. S 6 UV/Vis spectra of samples withdrawn in the time course (red to blue coloration) of a DHN solution (25 mL) irradiated (> 385 nm) in presence of methylene blue (MB) as photo-sensitizers under conditions as described in the main text.

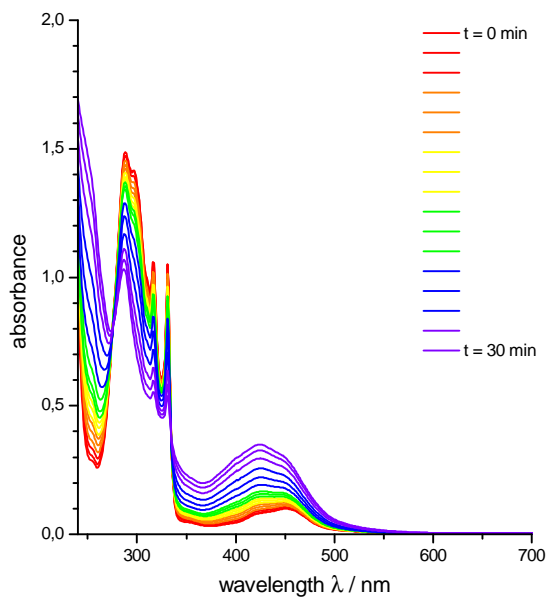


Fig. S 7 UV/Vis spectra of samples withdrawn in the time course (red to blue coloration) of a DHN solution (25 mL) irradiated (> 385 nm) in presence of $[\text{Ru}(\text{bpy})_3]\text{Cl}_2$ as photo-sensitizers under conditions as described in the main text.

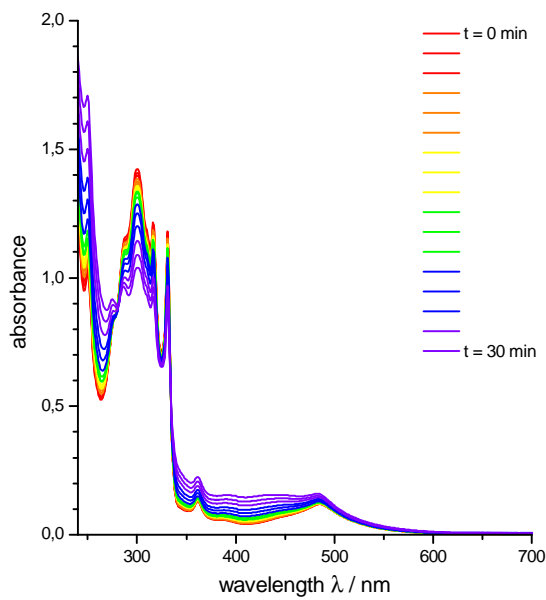


Fig. S 8 UV/Vis spectra of samples withdrawn in the time course (red to blue coloration) of a DHN solution (25 mL) irradiated (> 385 nm) in presence of $[\text{Ru}(\text{AT})_2]\text{PF}_6$ as photo-sensitizers under conditions as described in the main text.

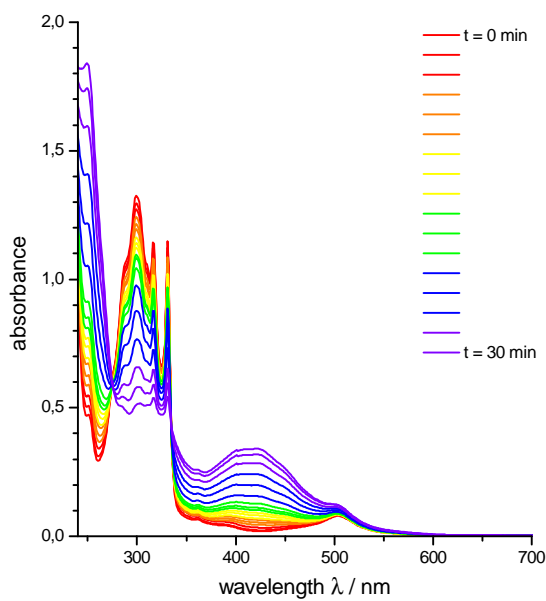


Fig. S 9 UV/Vis spectra of samples withdrawn in the time course (red to blue coloration) of a DHN solution (25 mL) irradiated ($> 385 \text{ nm}$) in presence of $[\text{Ru}(\text{ATT})_2]\text{PF}_6)_2$ as photo-sensitizers under conditions as described in the main text.

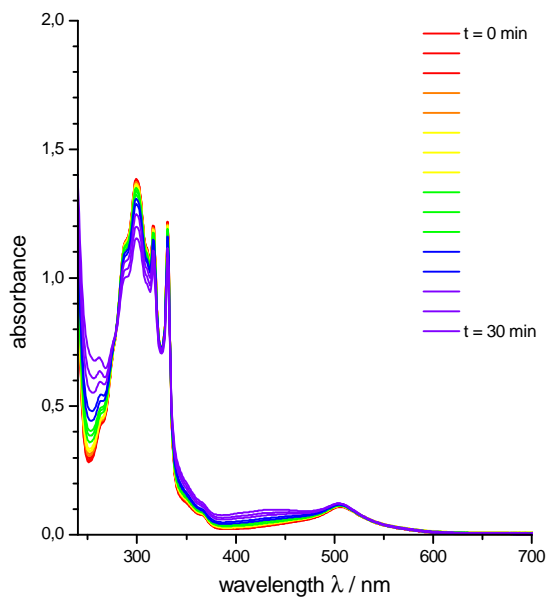


Fig. S 10 UV/Vis spectra of samples withdrawn in the time course (red to blue coloration) of a DHN solution (25 mL) irradiated ($> 385 \text{ nm}$, liquid NaNO_2 filter) in presence of $[\text{Ru}(\text{MeATT})_2]\text{PF}_6)_4$ as photo-sensitizers under conditions as described in the main text.

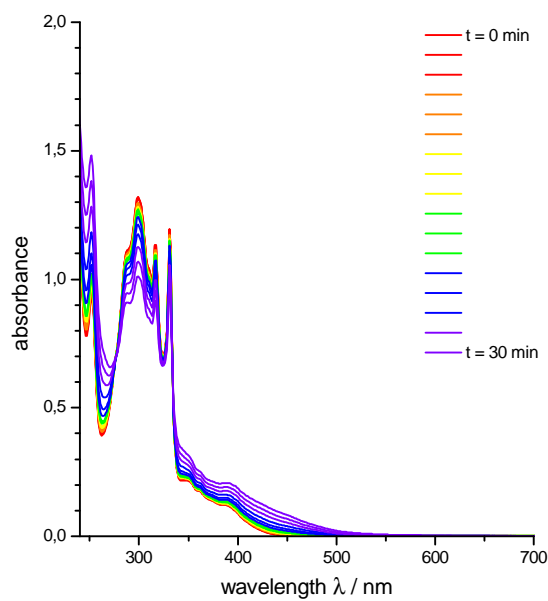


Fig. S 11 UV/Vis spectra of samples withdrawn in the time course (red to blue coloration) of a DHN solution (25 mL) irradiated (> 385 nm) in presence of $[\text{Zn}(\text{ATT})_2]\text{[PF}_6\text{]}_2$ as photo-sensitizers under conditions as described in the main text.

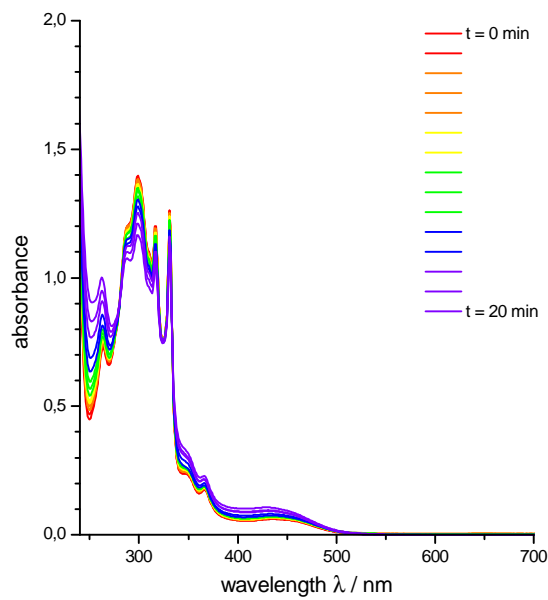


Fig. S 12 UV/Vis spectra of samples withdrawn in the time course (red to blue coloration) of a DHN solution (25 mL) irradiated (> 385 nm) in presence of $[\text{Zn}(\text{MeATT})_2]\text{[PF}_6\text{]}_4$ as photo-sensitizers under conditions as described in the main text.

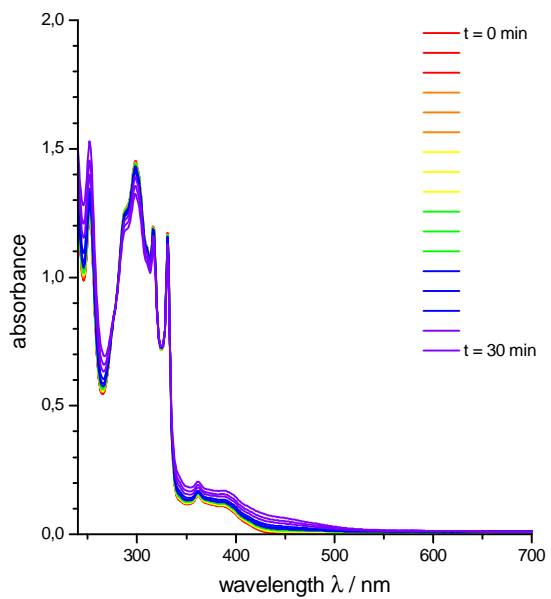


Fig. S 13 UV/Vis spectra of samples withdrawn in the time course (red to blue coloration) of a DHN solution (25 mL) irradiated (> 385 nm) in presence of the ATT ligand alone as photo-sensitizers under conditions as described in the main text..

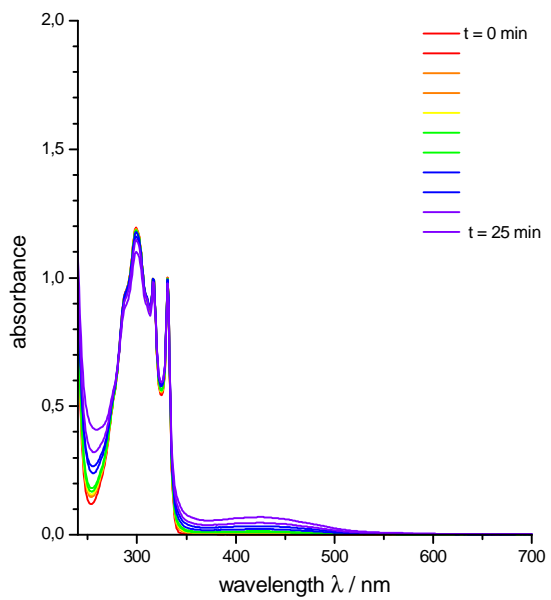


Fig. S 14 UV/Vis spectra of samples withdrawn in the time course (red to blue coloration) of a DHN solution (25 mL) irradiated (> 385 nm) without any sensitizer. Note the slight auto-sensitization capability by unavoidable Juglone traces.

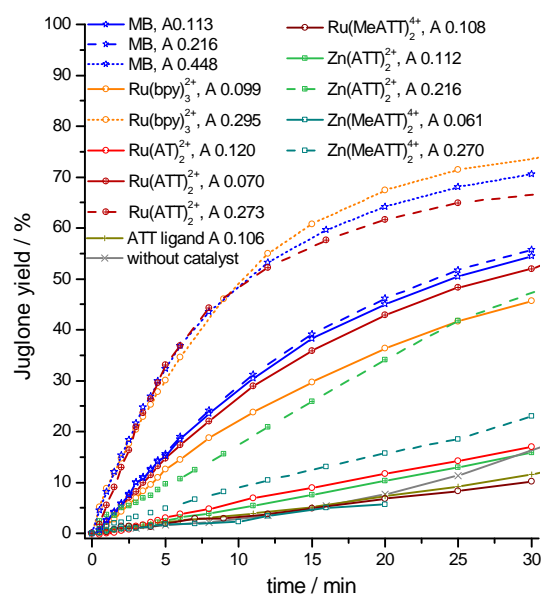


Fig. S 15 Reaction kinetics for the product, Juglone, with different photo-sensitizers employed as calculated from the increase of absorbance at λ 427 nm.

4.2 Limonene and 2-methylnaphthalene irradiation experiments

4.2.1 Photooxidation of limonene

Table S 1 Compilation of the photooxidation results for limonene from literature^{[6], [7], [8], [9], [10], [11]} and calculated average (thereby not distinguishing between the hydroperoxide and the alcohol resulting after treatment with reducing agents)

Ref. (method, R-group)	I ^a	II ^a	III ^a	IV ^a	V ^a	VI ^a
[6] (NMR, R=OH)	34	10	5	10	21	20
[7] (GC, R=OH)	40.1	5.8	4.0	8.5	21.0	20.6
[7] (GC, R=H)	33.5	6.4	4.0	9.4	25.8	20.9
[8a] (GC, R=H)	31	11	3	10	25	21
[8b] (GC, R=H)	34	10	4	9	23	19
[9] (GC, R=H)	34	10	5	10	21	20
[9c] ^b (GC, R=H)	40±2	11±1	2.5±0.5	7	20	19±1
[10] (GC, R=H)	30	7	3	8	26	23
[11] (GC, R=H)	37.7	9.1	4.5	9.1	18.1	21.1
[11] (HPLC, R=OH)	34.9	8.9	5.7	10.7	20.0	19.8
Average±Std. Dev. (1σ)	36±4	9±2	4±1	9±1	22±3	21±2
OCl ⁻ /H ₂ O ₂ ^[8]	34	9.5±0.5	7	9.5±0.5	23±1	18
μ-wave discharge ^{9c}	41	9	3	7	22	18

^a Note that the compound numbering scheme is *not* consistent within the different references.

^b Comparable experiments in this reference were summarized by arithmetic averaging.

Table S 2 Observed product distribution (without explicit assignment) for own photooxidations of (+)-limonene

Compound	Method	Distribution / %					
Zn(ATT) ₂ ²⁺ (1)	NMR ^a (<i>i.e.</i> Fig 19)	34	12	6	8	23	17
	GC (R=H)	37	7	3	6	29	18
Zn(MeATT) ₂ ²⁺ (2)	NMR ^a	31	14	7	9	23	16
Ru(ATT) ₂ ²⁺ (4)	NMR ^b	40	8	4	7	21	16
	GC (R=H)	39	10	5	9	21	16
2 nd batch	GC (R=H)	36	8	5	7	25	19
Ru(MeATT) ₂ ⁴⁺ (5)	NMR ^a	33	12	6	9	23	18
Methylene-blue	NMR ^a (<i>i.e.</i> Fig 20)	37	11	4	9	22	18
	GC (R=H)	38	8	4	9	25	16

^a Traces of unknown by-product observed. ^b About 4% of the unknown by-product observed.

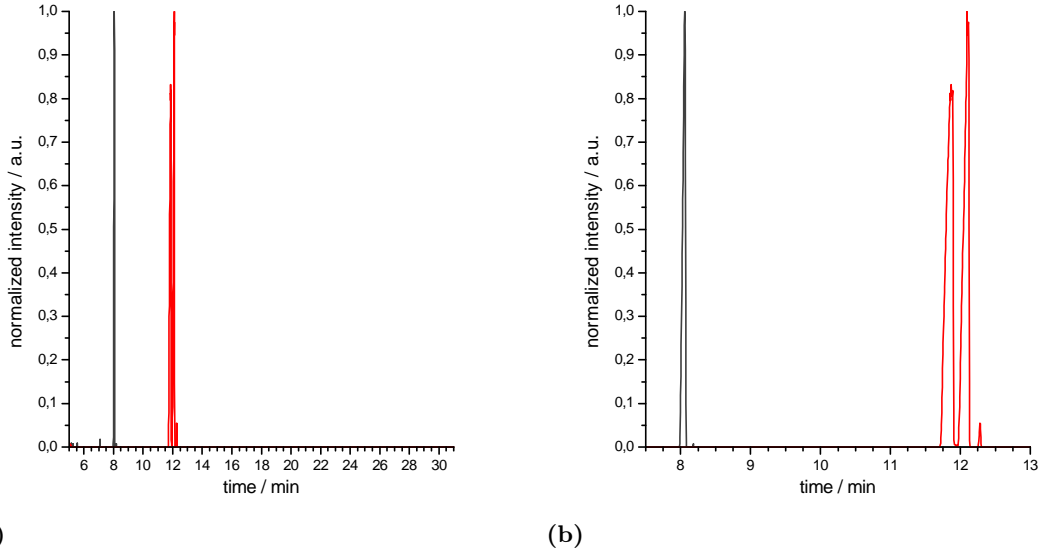


Fig. S 16 GC traces ((a), full; (b), zoom in region of interest) of neat (+)-limonene (dark grey) and mixture of (−)-carveol isomers (red), i.e. *cis* (compd. **III**) and *trans* (compd. **IV**). Unassigned ratio: 53:47 % (by GC and NMR).

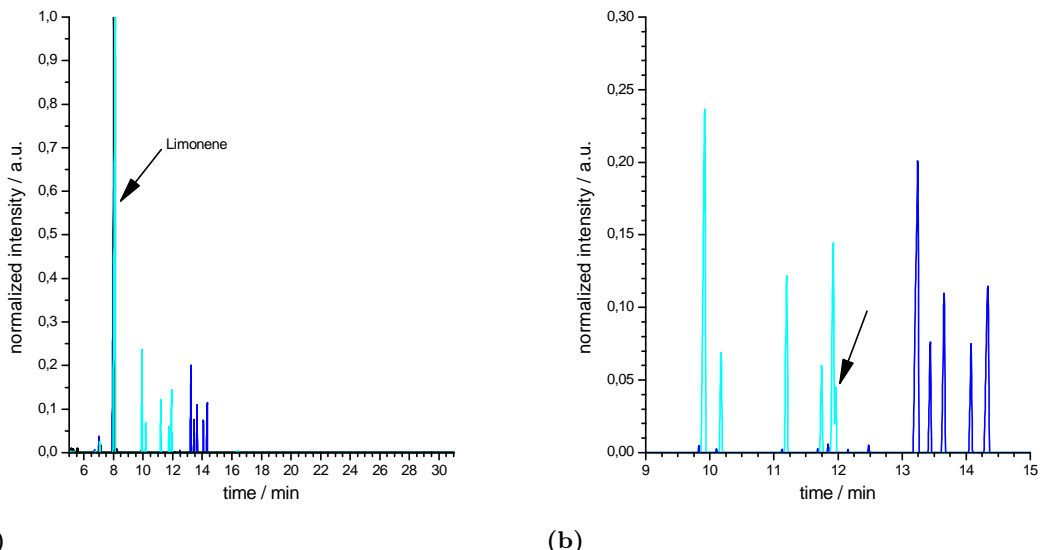


Fig. S 17 GC traces ((a), full view; (b), zoom in region of interest) of (+)-limonene direct after irradiation with methylene blue as sensitizer in MeCN-*d*₃ (blue trace) and after reduction with NaBH₄ (cyan). Note the arrow in the magnified chromatogram (panel b) indicating the barely separated 6th signal evolving from the five observed hydroperoxide signals after reduction and the limonene signal (black, almost indistinguishable overlay at about *t*_{ret.} = 8 min) in the full chromatogram (panel a).

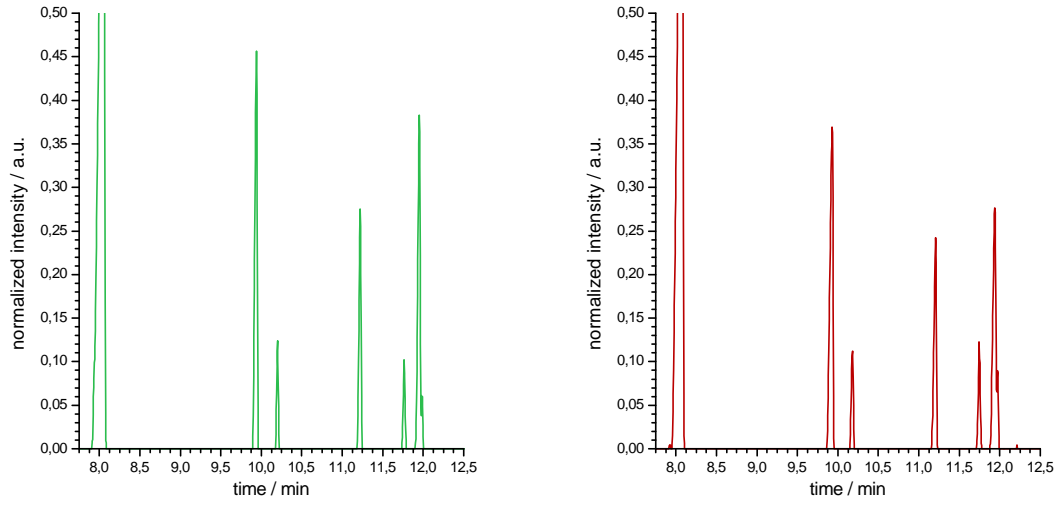


Fig. S 18 GC traces (region of interest only) from irradiation experiments with (+)-limonene in MeCN-*d*₃ using [Zn(ATT)₂][PF₆]₂ ((a), green) and [Ru(ATT)₂][PF₆]₂ ((b), maroon) respectively, as sensitizers after reduction of the reaction mixture.

Table S 3 Summary of GC retention times (in ascending order; see section 1.1.1 for GC parameters) for the products resulting from the photooxidation of (+)-limonene and reduction of the reaction mixture afterwards, respectively

Signal	Retention time / s	Std. dev. (1σ)
(+)-limonene	483.8	0.6
1 st Alcohol	596.6	0.8
2 nd Alcohol	611.6	0.6
3 rd Alcohol	673.1	0.5
4 th Alcohol	705.2	0.4
5 th Alcohol	717.0	0.5
6 th Alcohol	718.5	0.2
1 st (-) -carveol <i>cis/trans</i> -mix (compd. III/IV)	712.2	n.a.
2 nd (-) -carveol <i>cis/trans</i> -mix (compd. III/IV)	725.7	n.a.
1 st Hydroperoxide	800.2	1.1
2 nd Hydroperoxide	811.7	0.6
3 rd Hydroperoxide	824.7	0.9
4 th Hydroperoxide	849.0	0.1
5+6 th Hydroperoxide	865.1	0.8

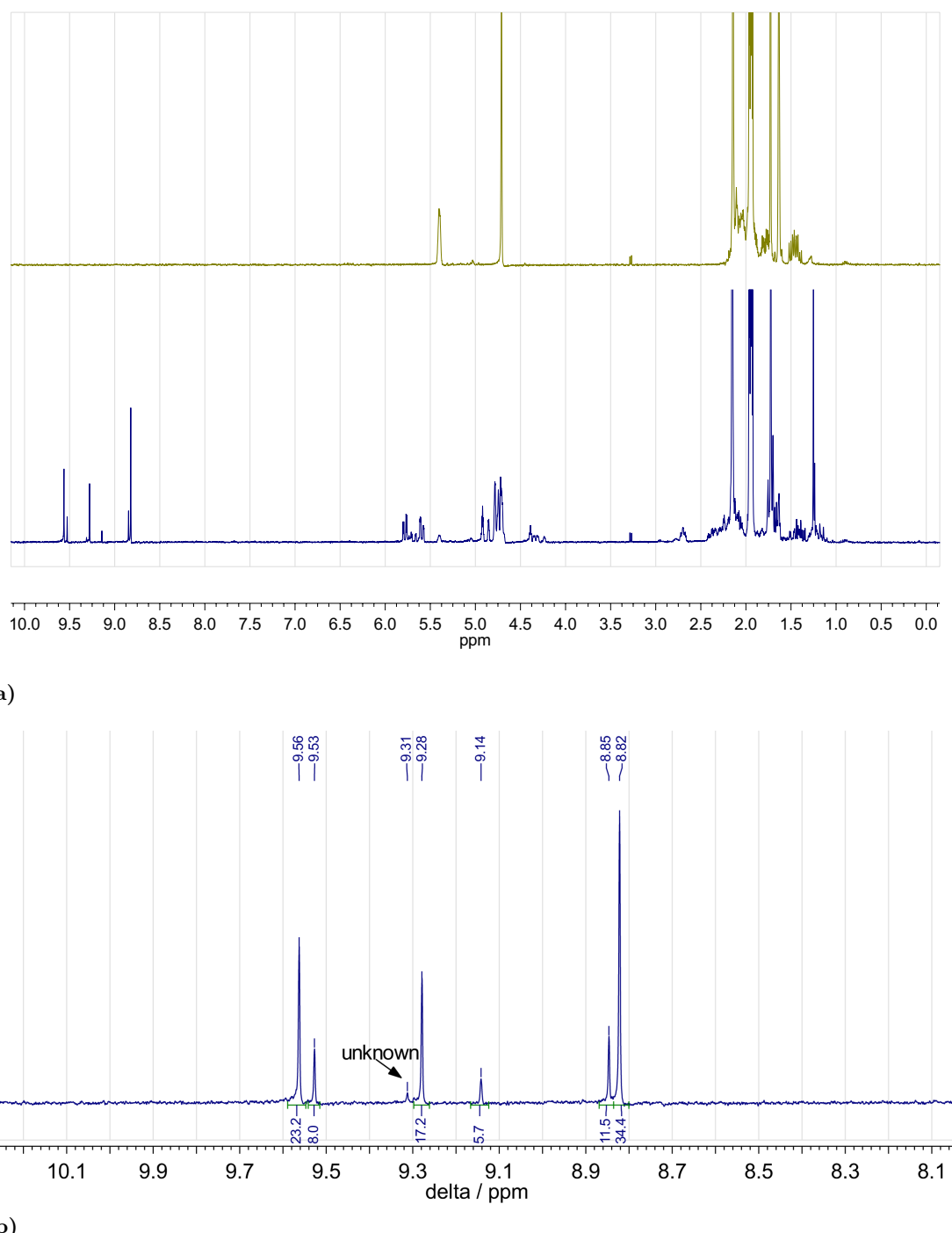
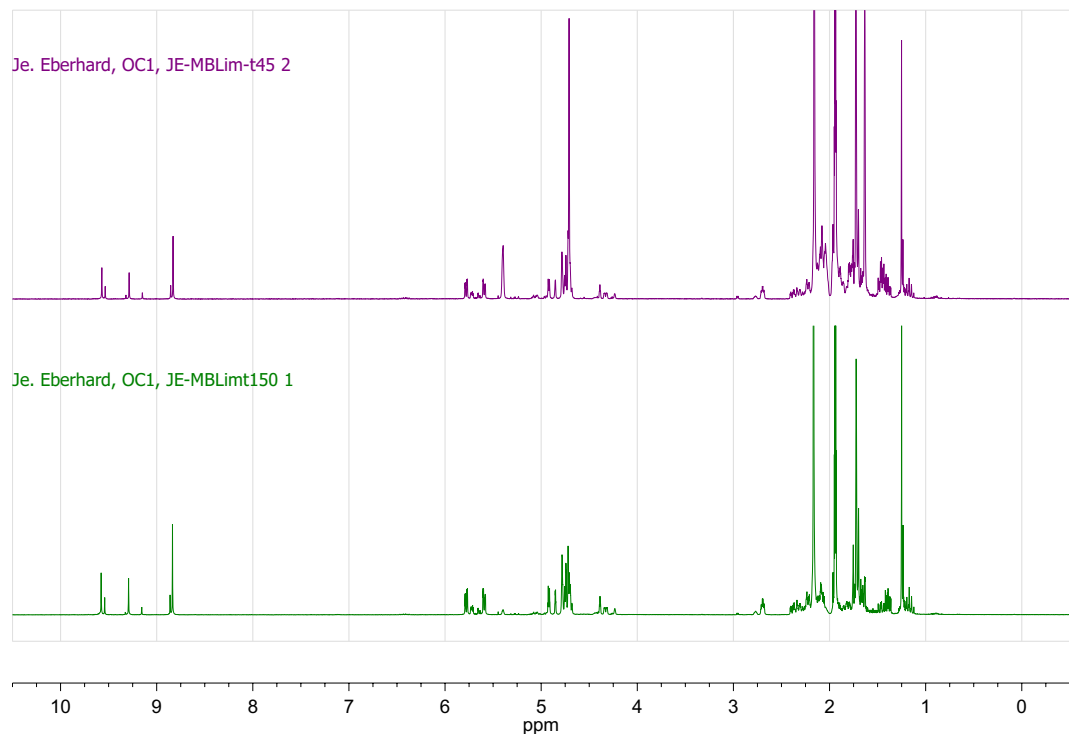
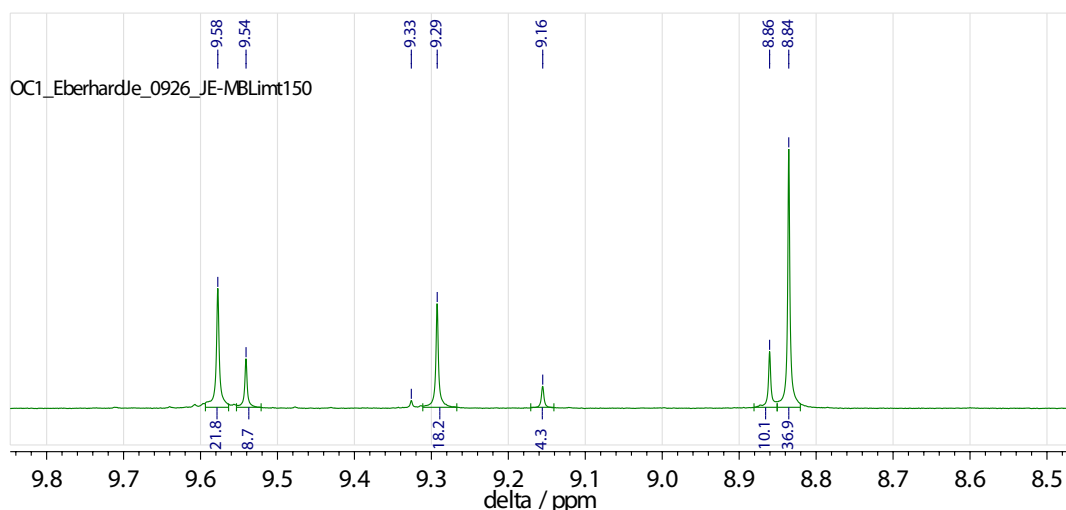


Fig. S 19 Exemplary spectra of an irradiation experiment (400 W Hg lamp) with (+)-limonene (30 mM) as substrate in MeCN- d_3 and $[\text{Zn}(\text{ATT})_2][\text{PF}_6]_2$ as sensitizer in this case: Before (a; dark yellow, top) and after irradiation (a; dark blue, bottom) and the magnification of the aforementioned spectra (b) in the region of the $-OOH$ resonances. The integrals (normalized to 100 %) are therefore a direct measure for the product distribution.



(a)



(b)

Fig. S 20 Reference irradiation (Rayonet® reactor) of (+)-limonene (30 mM) with methylene blue as sensitizer in MeCN-*d*₃: full spectra after 45 min (a; top) and 150 min (a; bottom) and the magnification of last spectra (panel b, as in Fig S19).

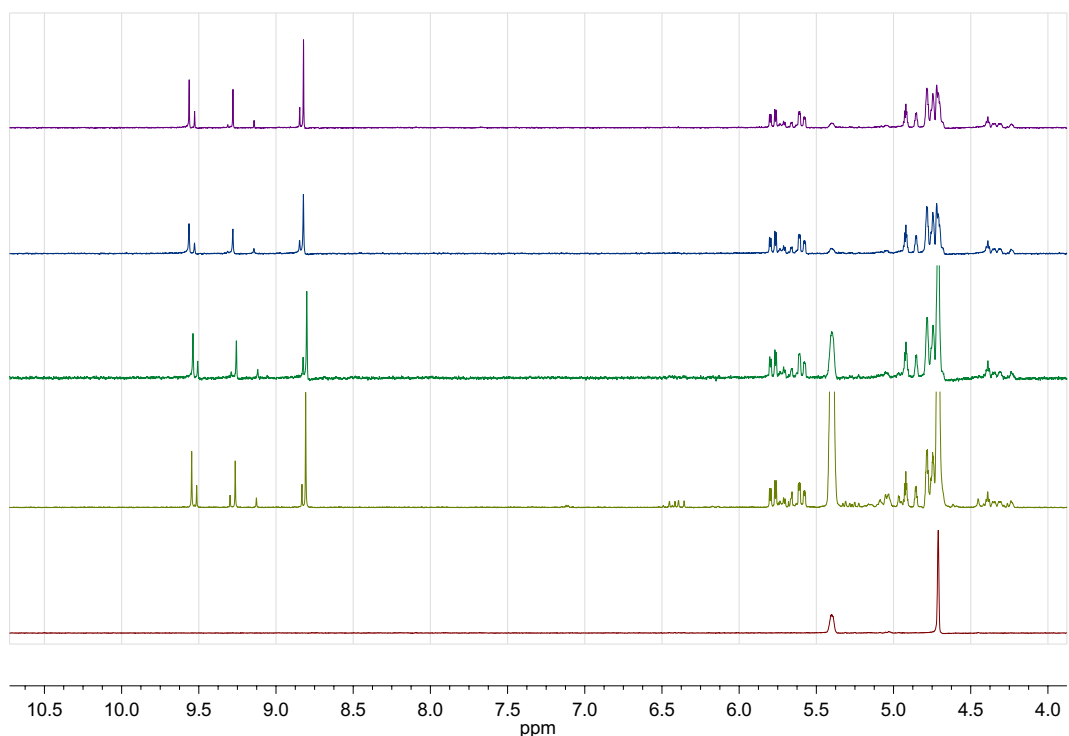


Fig. S 21 NMR spectroscopic (300 MHz) comparison of different catalysts $[\text{Zn}(\text{ATT})_2][\text{PF}_6]_2$ (violettt), $[\text{Zn}(\text{MeATT})_2][\text{PF}_6]_4$ (blue), $[\text{Ru}(\text{MeATT})_2][\text{PF}_6]_2$ (cyan-green), and $[\text{Ru}(\text{ATT})_2][\text{PF}_6]_2$ (dark yellow) in the photooxidation of (+)-limonene in $\text{MeCN}-d_3$. A sample spectra of (+)-limonene before irradiation ($t = 0$, maroon) is also included for comparison. Irradiation was performed with an 400 W high pressure Hg lamp (75 min, w. NaNO_2 liquid filter) or a Rayonet® reactor (60 min) in case of $[\text{Ru}(\text{ATT})_2][\text{PF}_6]_2$ which converted all limonene in the previous experiment within the time span.

4.2.2 Attempted photooxidation of 2-methylnaphthalene

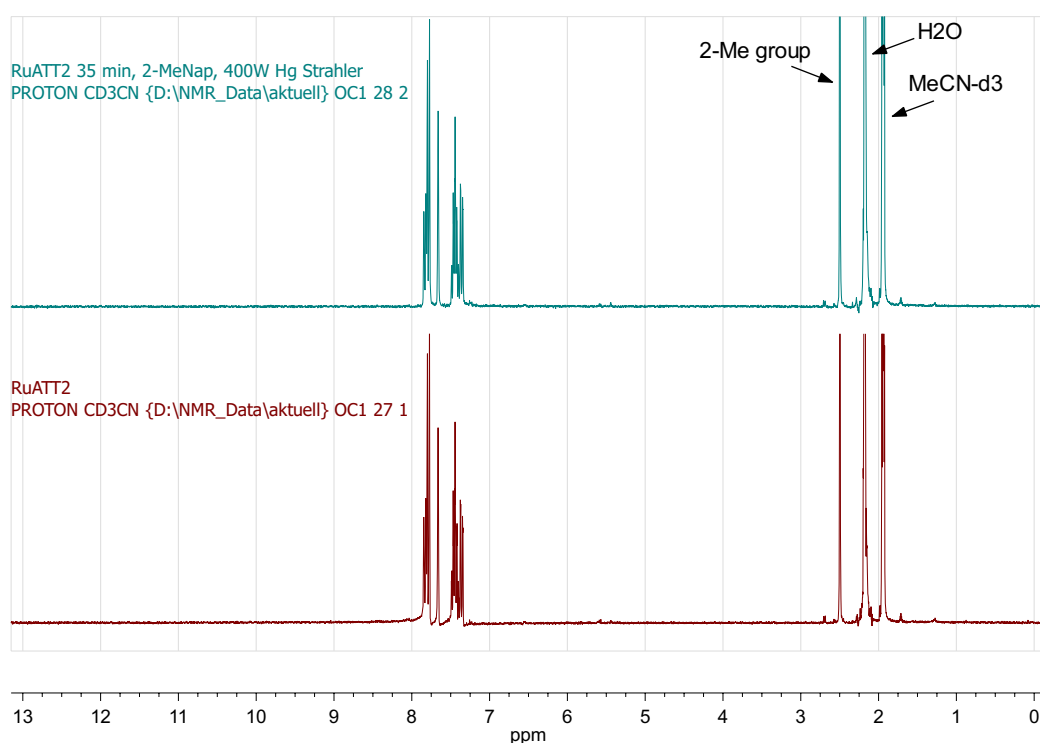


Fig. S 22 Exemplary NMR (300 MHz, MeCN-*d*3) (slightly magnified) of an irradiated sample of 2-methylnaphthalene (0.012 M with [Ru(ATT)₂][PF₆]₂ (7.5 µM, abs. (A) 0.38 at 504 nm) photocatalyst in this case). No aldehyde signal^[6] was observed regardless of lamp employed (400 W Hg lamp w. filter, 35 min, or Rayonet® reactor, 140 min).

4.3 Actinometry

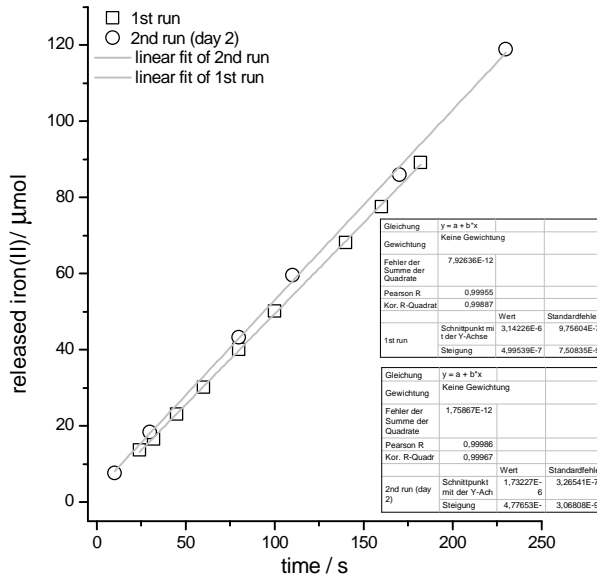


Fig. S 23 Ferrioxalate actinometry (0.012 M)^[12] for determination of the photon flux in our semi-preparative setup. We used the ferrioxalate ammonium salt (98 %, Alfa Aesar) in $0.05\text{ M H}_2\text{SO}_4$. Withdrawn sample volume was $0.98 \pm 0.02\text{ ml}$ (1 ml syringe) at given time which was immediately added to 5 ml of the buffered (sodium acetate/ H_2SO_4) phenanthroline "developer" solution and filled up later ($> 5\text{ min}$) to a final volume of 20 ml, or 25 ml respectively, in a corresponding volumetric flask. The blank negative control had absorption values below 0.042 at 510 nm.

The energy of a photon E_p (note $\text{W} = \text{J s}^{-1}$) is given by

$$E_p = h \nu = \frac{h c}{\lambda} \quad (1)$$

with Planck constant $h = 6.626\,07 \times 10^{-34}\text{ J s}$, speed of light $c = 2.997\,92 \times 10^8\text{ m s}^{-1}$, frequency ν in s^{-1} and wavelength λ in m.

At a given irradiance E_e (in W m^{-2}) the number of photons N_p for the wavelength λ (now for convenience in nm) per area and second can be calculated:

$$N_p = E_e / E_p = \frac{E_e \lambda \times 10^{-9}}{h c} = E_e \lambda 5.03412 \times 10^{15} (\text{m}^{-2} \text{s}^{-1}) \quad (2)$$

The molar photon flux Φ_E (in Einstein $\text{m}^{-2} \text{s}^{-1}$) can be obtained through division by the Avogadro constant $N_A = 6.022\,14 \times 10^{23} \text{ mol}^{-1}$.^[13]

$$\Phi_E = N_p / N_A \quad (3)$$

Taken together, this leads to the usual given expression for converting irradiance (or radiant flux, if not related to an area) from power-based to quantum-based units.^[12, 13]

$$\Phi_E (\text{Einstein m}^{-2} \text{s}^{-1}) = E_e (\text{W m}^{-2}) \times \lambda (\text{nm}) \times 8.35935 \times 10^{-9} \quad (4)$$

Based on some assumptions an irradiance value (in mW cm^{-2}) can be derived as mentioned in the main text. However, this can only be approximated, since the high-pressure Hg lamp act as broadband source with some distinct spectral line emission characteristics. Some typical power values were adopted from literature sources and compiled for the 385-800 nm range in Table S4. [12–14]

Table S 4 Summary of spectral power values for comparable Hg lamps from literature.

	Ref. [13] 400 W ^a lamp		Ref. [14] 450 W ^a lamp
λ / nm	Power / W	λ / nm	Power / W
390-420	10	404.5	11.0
420-450	15	435.8	20.2
540-570	20	546.1	24.5
570-600	17	578.0	20.0
		1014.0	10.5
		1128.7	3.3
		1367.3	2.6
Sum	72	Sum	92.1 ^b
F^c	0.49	F^c	0.34

^a Electrical power; energy conversion efficiency about 30-40 % from that ~60 % in the UV and ~40 % in the VIS range (see Ref. [13]). ^b 75.7 W up to 600 nm. ^c Fraction (F) usable for ferrioxalate actinometry.

The quantum yield of Fe^{II} ($\Phi_{\text{Fe(II)}}$) production was taken from the literature and assumed to be dominated (1st approximation) by the 405 and 436 nm Hg lines with $\Phi_{\text{Fe(II)}}$ ~1.1. [12] The usable light fraction for actinometry of the total spectral power is given in Table S4. We used $F = 0.34$ due to consideration of the considerable (N)IR (heat) emission of high pressure Hg lamps. (2nd approximation and justification for water heat shield), which provides than by use the following equation: [12]

$$\Phi_e(\text{Einstein s}^{-1}) = \frac{n_{\text{Fe(II)}}}{t \Phi_{\text{Fe(II)}} F} \quad (5)$$

A photon flux (in Einstein s^{-1}) of $1.31 \pm 0.03 \times 10^{-6} \text{ Es}^{-1}$ for the VIS-NIR range. For the relation to an area we consider the round bottom flask as perfect spheric in shape (at least for the bottom part where the reaction takes place). By this, surface area and volume can be calculated:

$$V = \frac{1}{6} \pi d^3 \quad \text{and} \quad A = \pi d^2 \quad (6)$$

Assuming the manufacturer specified outer diameter (o.d.) of 51 mm for a 50 ml-round-bottom flask and 2 mm glass thickness, we obtain an inner diameter (d) of 49 mm (3rd approximation). The actual irradiated surface area (A_{irr}) containing the actinometer solution can be calculated by cross-multiplication from the start volumes of 32 and 22 ml used. Furthermore it is mandatory for any actinometry experiment to block straylight to negligible levels (we used black cardboard around the liquid filter solution for all experiments) and to assume total absorption of the incident photons (*i.e.* only the front side contributes, *viz.* half of the surface) which gives than 20 cm^2 and 13 cm^2 , respectively.

Finally the irradiance value (in mW cm^{-2}) can be calculated assuming the 436 nm Hg line as dominant (4^{th} approximation):

$$E_e(\text{mW cm}^{-2}) = \frac{\Phi_e(\text{Es}^{-1})}{\lambda(\text{nm}) \times A_{\text{irr}}(\text{cm}^2) \times 8.35935 \times 10^{-12}} \quad (7)$$

Which yields $22 \pm 4 \text{ mW cm}^{-2}$ in average for both runs.

4.3.1 Transmission of NaNO_2 filter solution

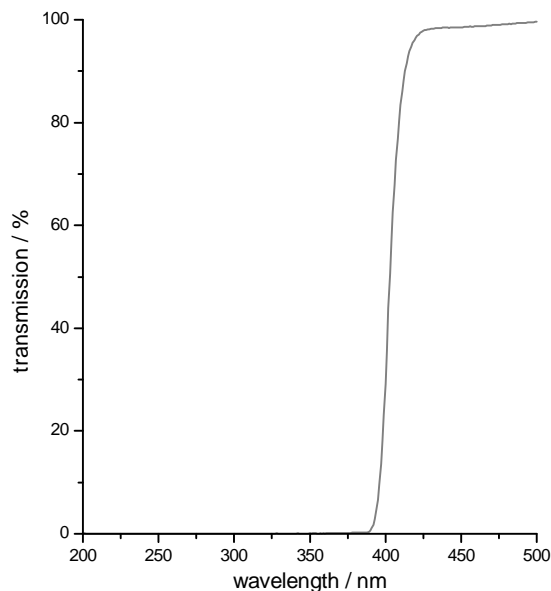


Fig. S 24 Transmission spectra of the aqueous NaNO_2 filter solution (0.72 M) after about 2 weeks of use.

5 Analytical data

5.1 NMR data of the zinc(II) complexes

5.1.1 $[\text{Zn}(\text{ATT})_2][\text{PF}_6]_2$ (1)

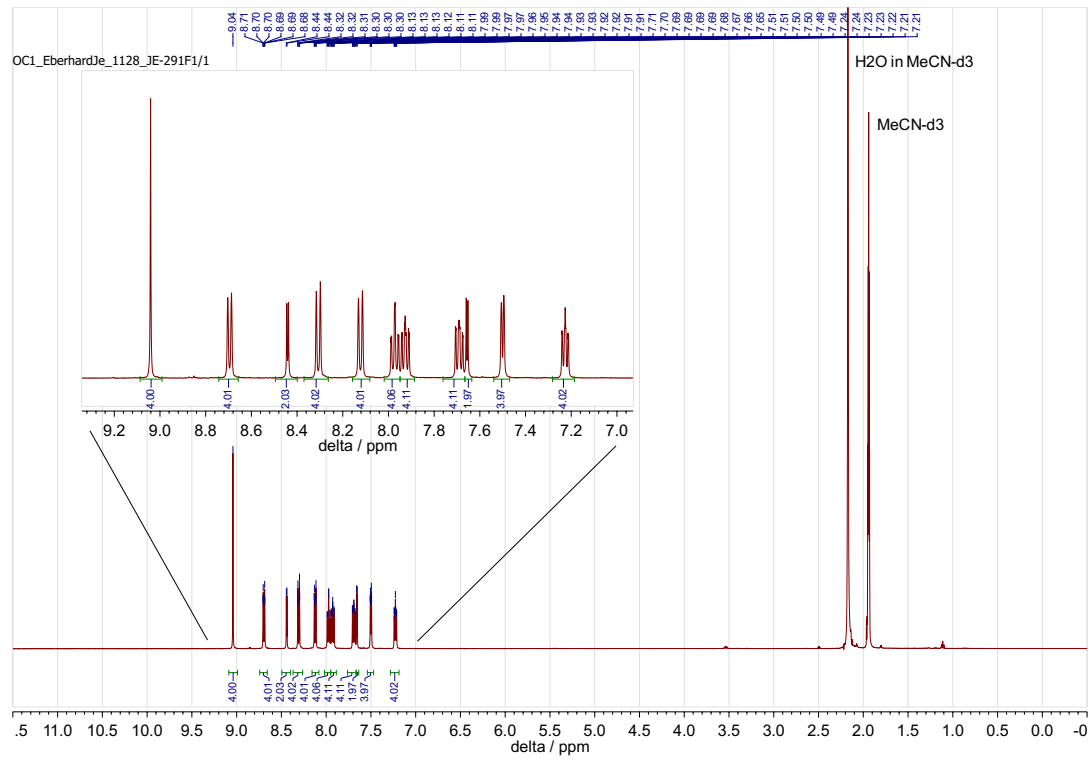


Fig. S 25 ^1H NMR data of $[\text{Zn}(\text{ATT})_2][\text{PF}_6]_2$ (**1**) in $\text{MeCN}-d_3$.

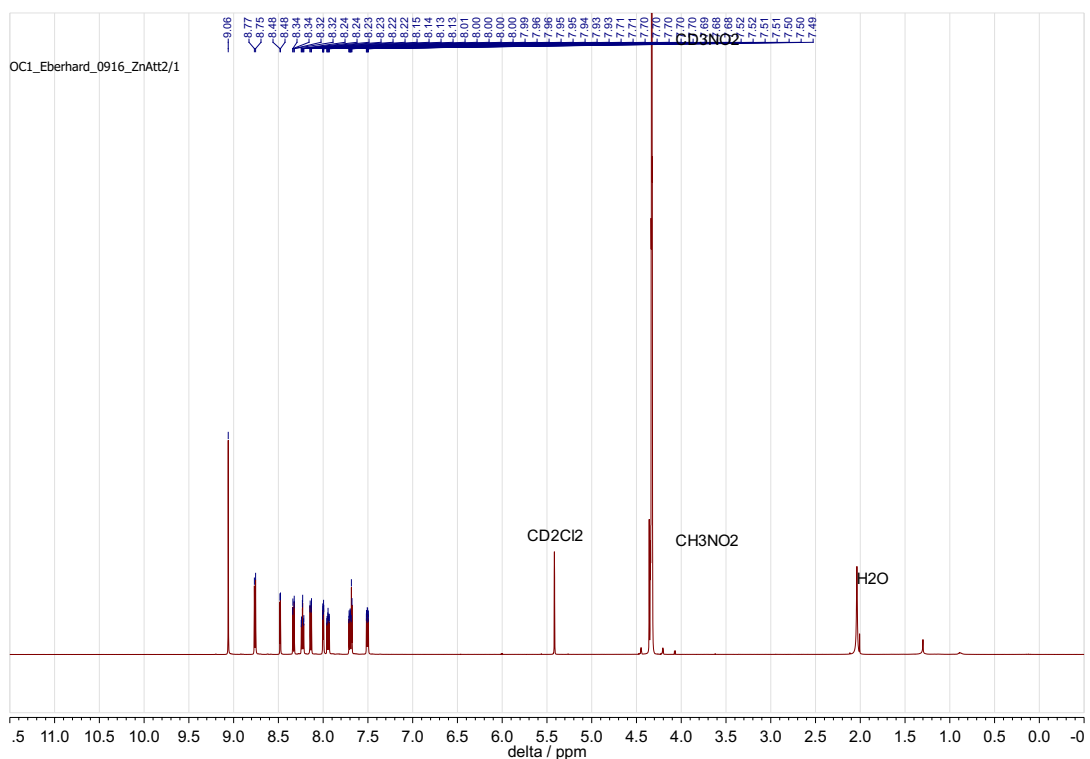


Fig. S 26 2nd ¹H NMR of [Zn(ATT)₂][PF₆]₂ (**1**) in CD₃NO₂/CD₂Cl₂ 4:1 (v/v).

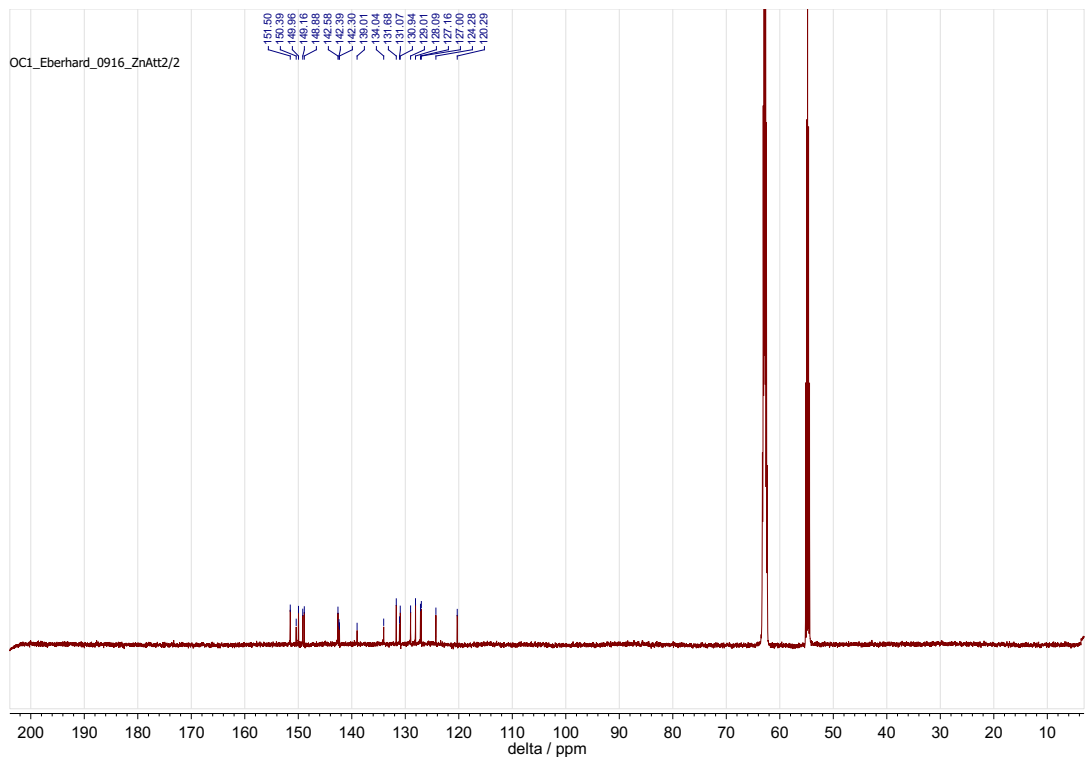


Fig. S 27 ¹³C NMR data of [Zn(ATT)₂][PF₆]₂ (**1**) in CD₃NO₂/CD₂Cl₂ 4:1 (v/v).

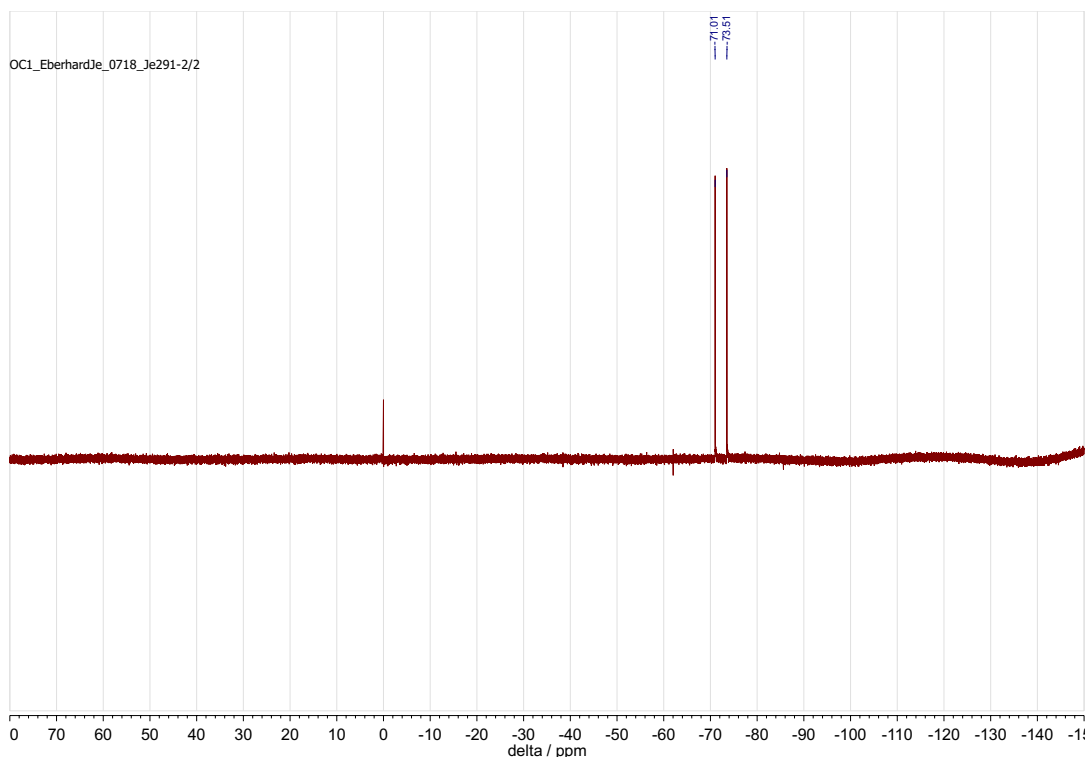


Fig. S 28 ¹⁹F NMR data of $[\text{Zn}(\text{ATT})_2]\text{[PF}_6\text{]}_2$ (**1**) in MeCN-*d*₃ with sealed capillary containing CFCl₃ (0 ppm) as internal standard in acetone-*d*6.

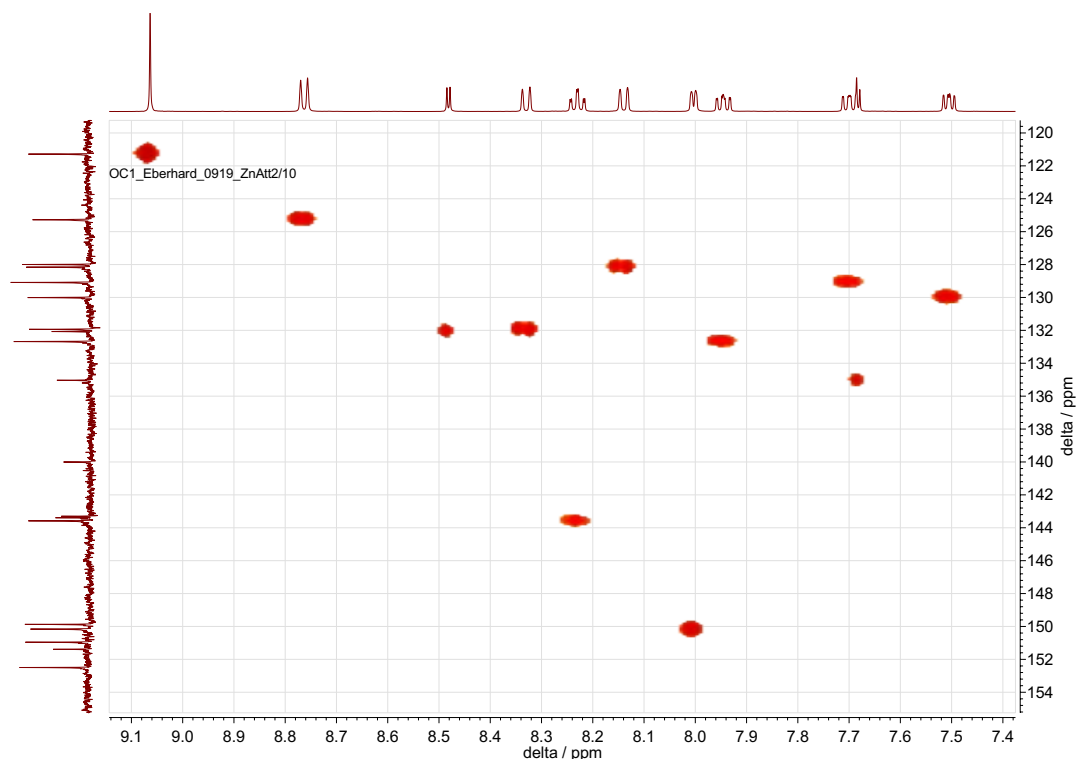


Fig. S 29 Zoom into the aromatic region of the HSQC data of $[\text{Zn}(\text{ATT})_2][\text{PF}_6]_2$ (**1**) in $\text{CD}_3\text{NO}_2/\text{CD}_2\text{Cl}_2$ 4:1 (v/v).

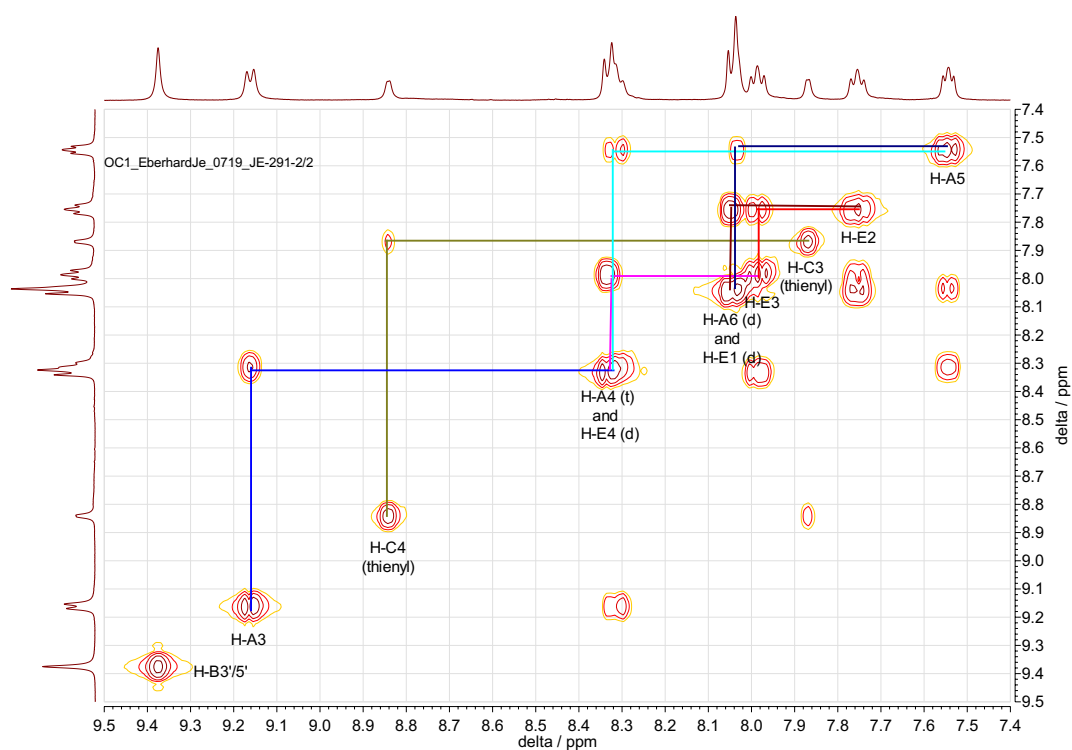


Fig. S 30 Zoom into the aromatic region of the COSY data of $[\text{Zn}(\text{ATT})_2][\text{PF}_6]_2$ (**1**) in $\text{DMSO}-d_6$.

5.1.2 $[\text{Zn}(\text{MeATT})_2][\text{PF}_6]_4$ (2)

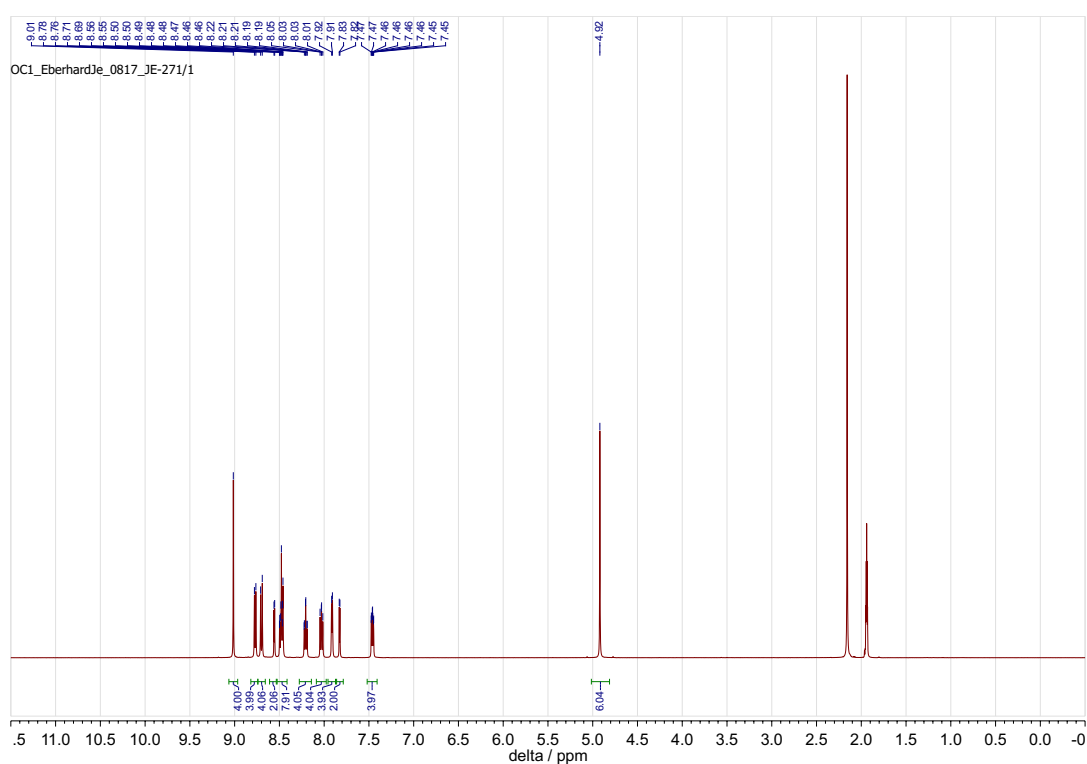


Fig. S 31 ^1H NMR data of $[\text{Zn}(\text{MeATT})_2][\text{PF}_6]_4$ (**2**) in $\text{MeCN-}d_3$.

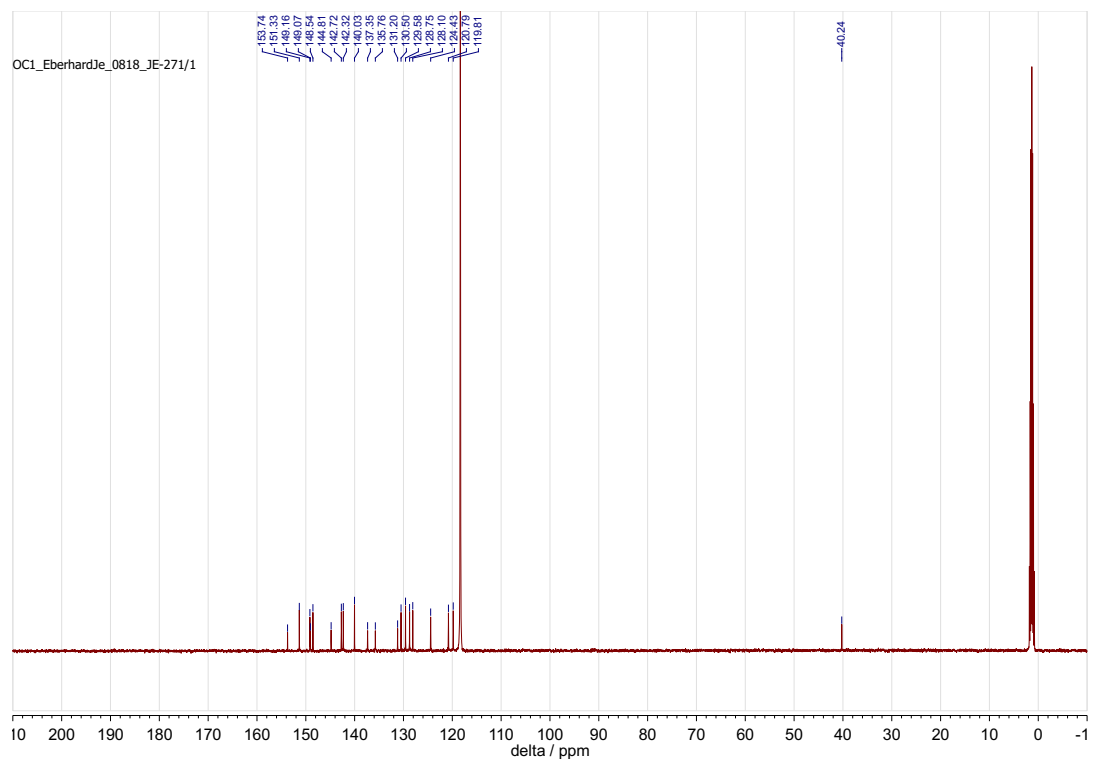


Fig. S 32 ^{13}C NMR data of $[\text{Zn}(\text{MeATT})_2][\text{PF}_6]_4$ (**2**) in $\text{MeCN}-d_3$.

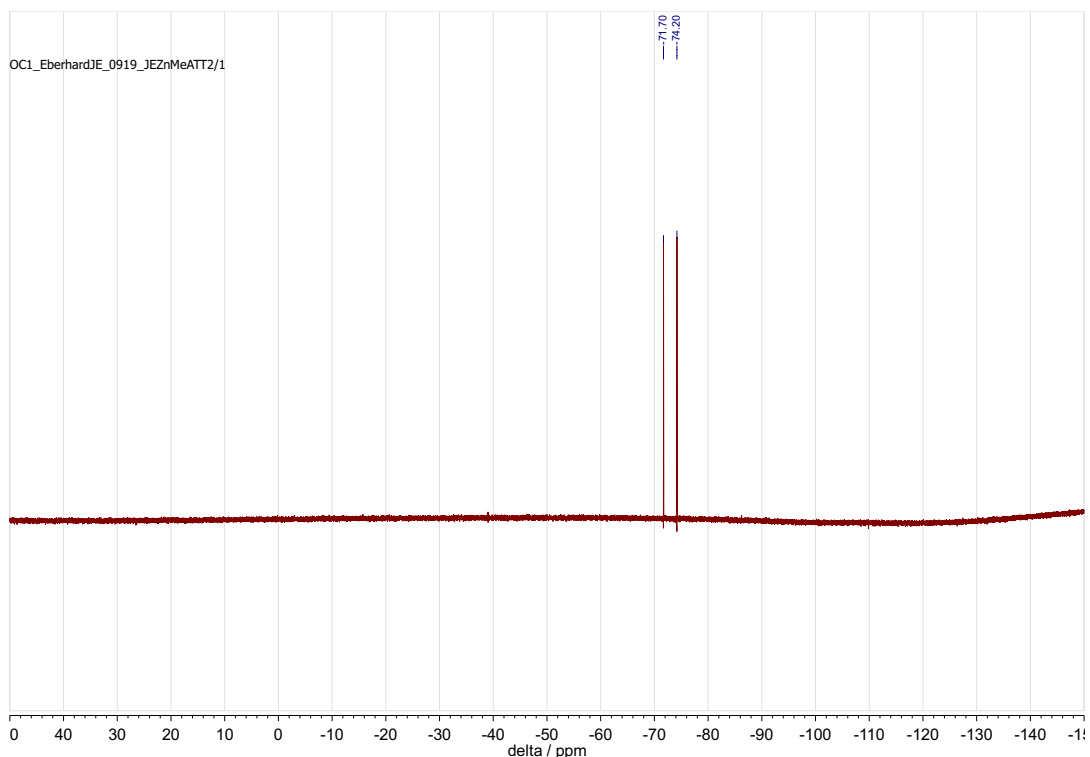


Fig. S 33 ¹⁹F NMR data of $[\text{Zn}(\text{MeATT})_2][\text{PF}_6]_4$ (**2**) in $\text{MeCN}-d_3$ (external calibration).

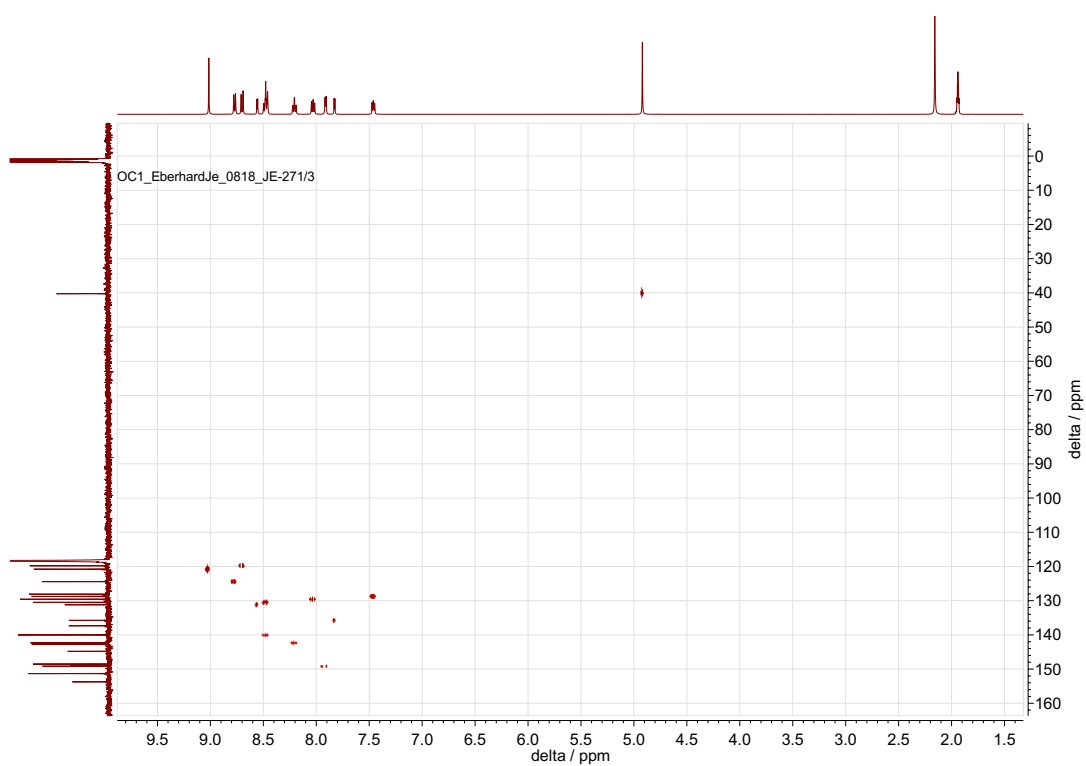


Fig. S 34 HMQC data of compound $[\text{Zn}(\text{MeATT})_2][\text{PF}_6]_4$ (**2**) in $\text{MeCN}-d_3$.

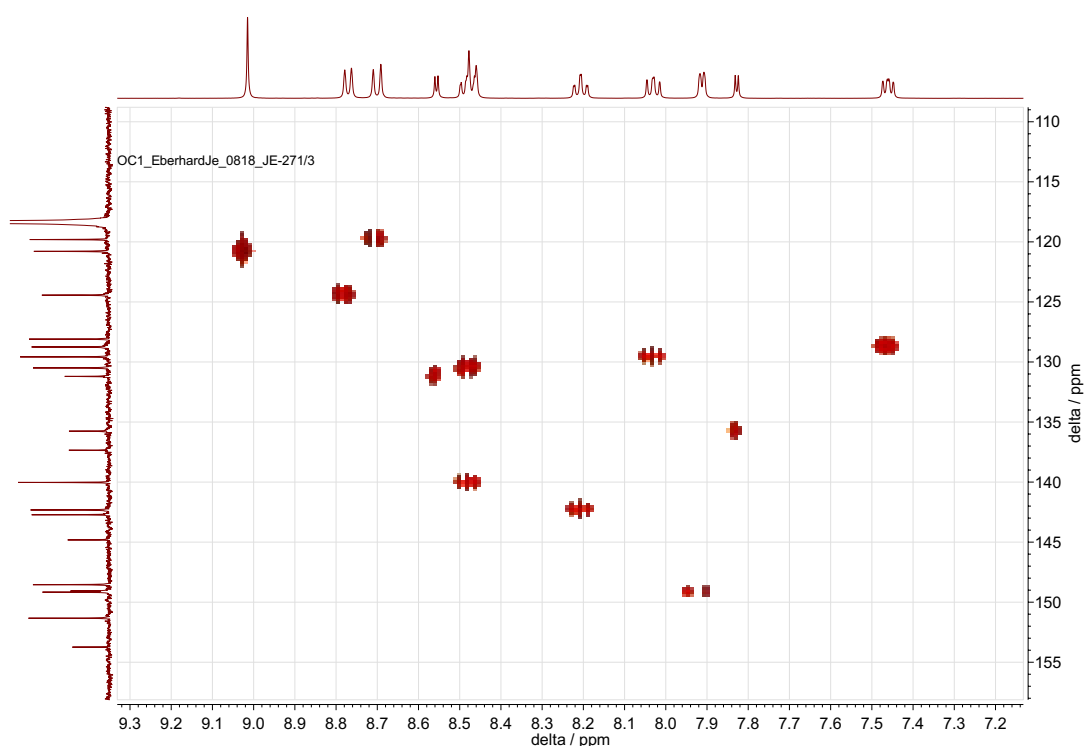


Fig. S 35 Zoom into the aromatic region of the HMQC data of $[\text{Zn}(\text{MeATT})_2][\text{PF}_6]_4$ (**2**).

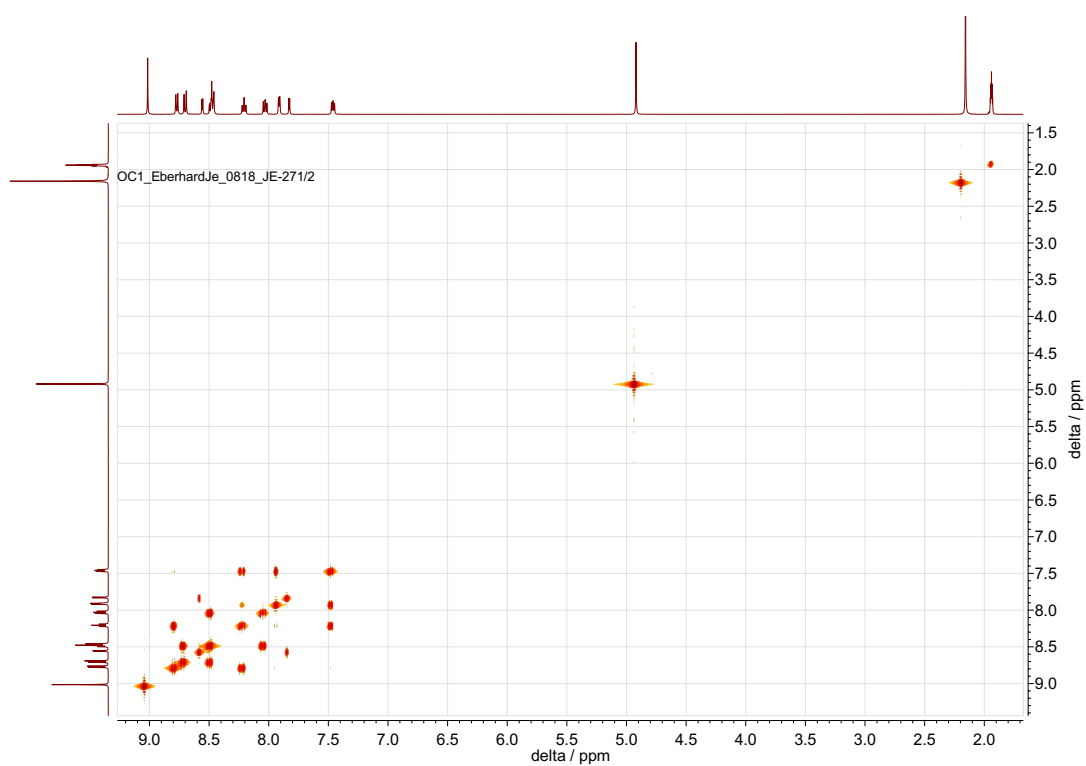


Fig. S 36 COSY data of compound $[Zn(\text{MeATT})_2][\text{PF}_6]_4$ (2) in $\text{MeCN}-d_3$.

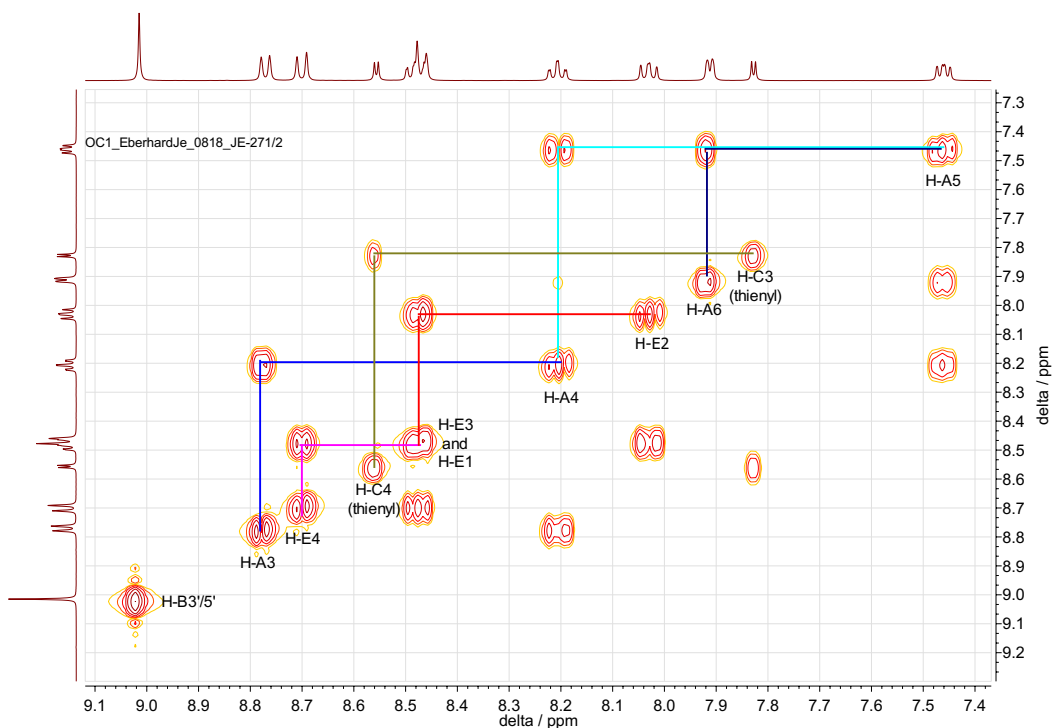


Fig. S 37 Zoom into the aromatic region of the COSY data of $[Zn(\text{MeATT})_2][\text{PF}_6]_4$ (**2**).

5.2 IR data

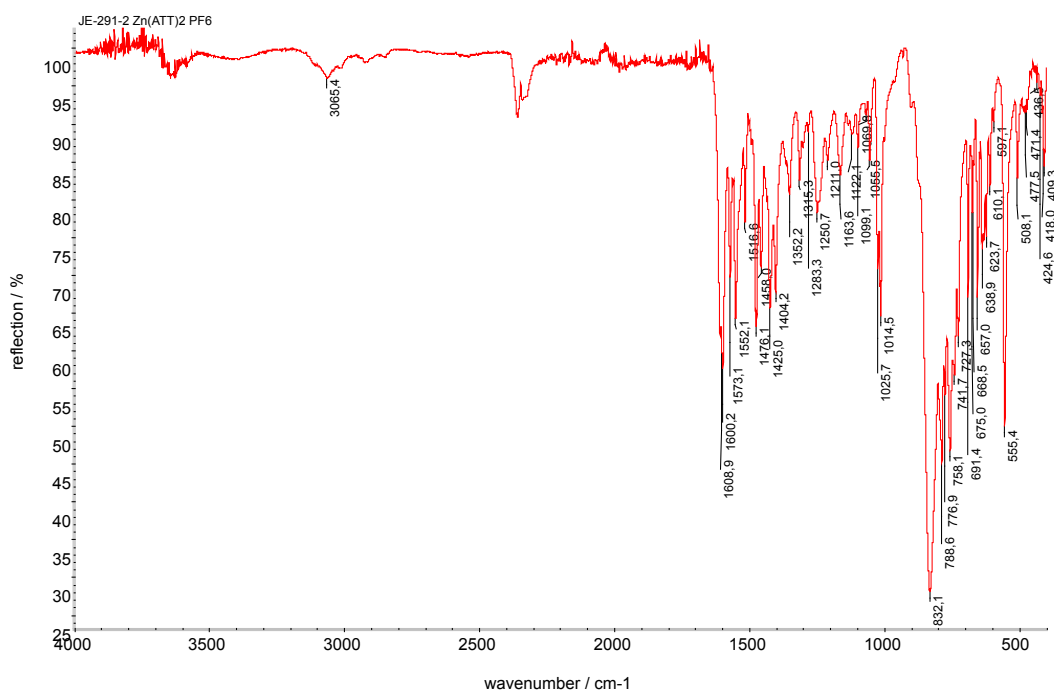


Fig. S 38 Infrared spectra (ATR) of $[\text{Zn}(\text{ATT})_2][\text{PF}_6]_2$ (**1**).

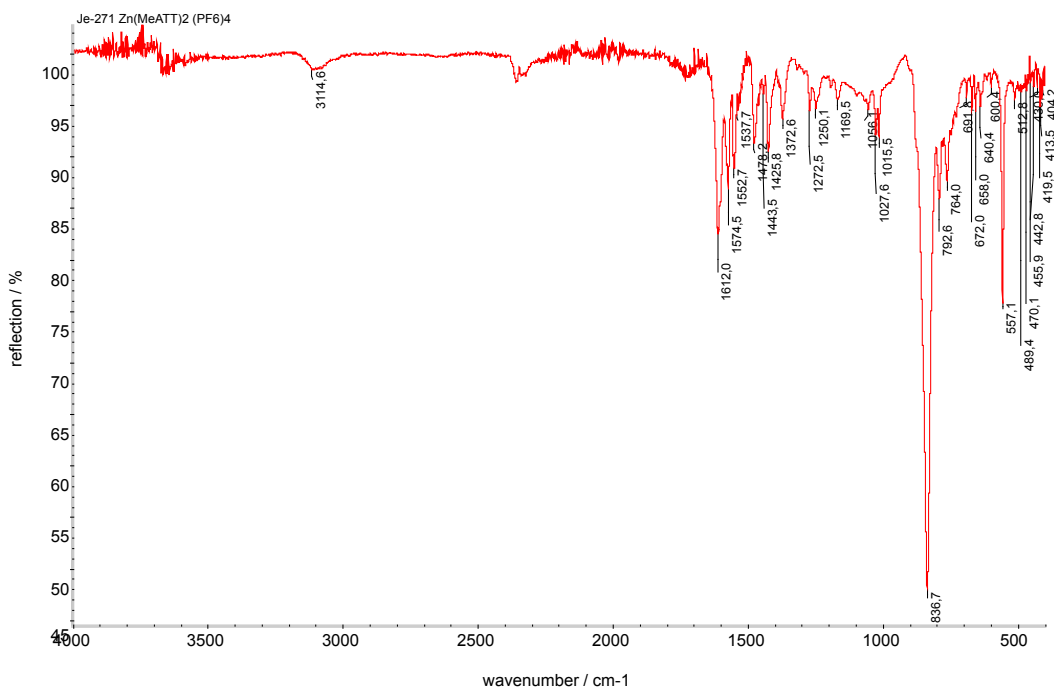


Fig. S 39 Infrared spectra (ATR) of $[\text{Zn}(\text{MeATT})_2][\text{PF}_6]_4$ (**2**).

5.3 MS data

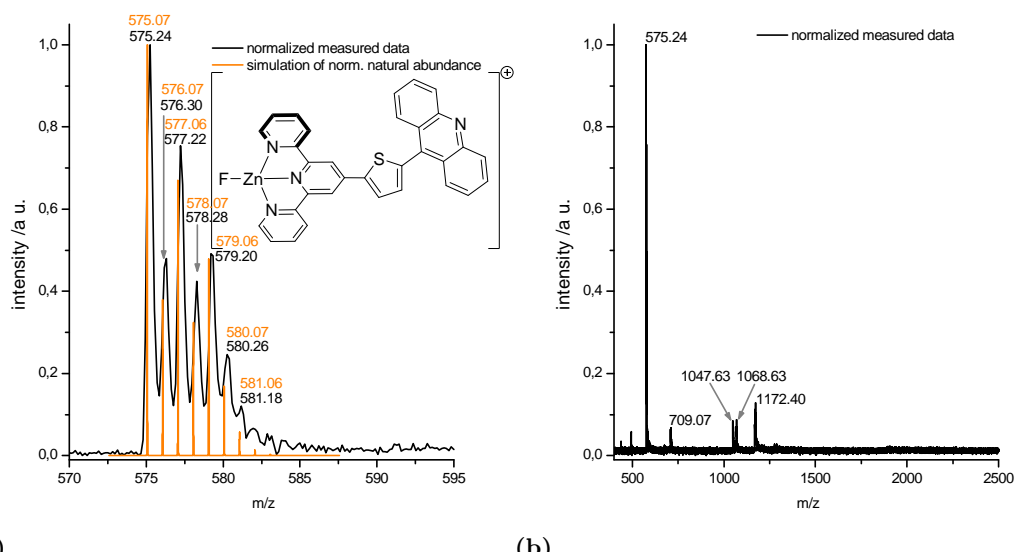
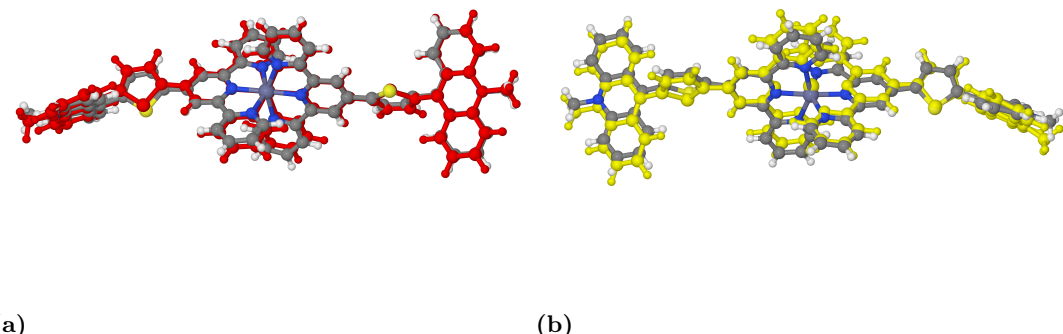


Fig. S 40 Magnification of the main peak in MALDI-ToF spectra (DCTB matrix) of $[Zn(ATT)_2][PF_6]_2$ (**1**). The peak corresponds to a $[M - ATT + F]^+$ fragment ion (calc, for $C_{32}H_{20}FN_4S\text{Zn}^+$: 575.07, found 575.24 (a) and full spectra (b)). The signals at 1047.63 and 1068.63 (avg.) might represent $[M - 2 PF_6 + e]^+$ and $[M - 2 PF_6 + F]^+$ pseudo-molecular ions, respectively (calc. 1048.21 and 1067.21, resp.). However, they are not well-resolved.

6 Computational methods

6.1 Comparison of X-ray data and calculated geometry

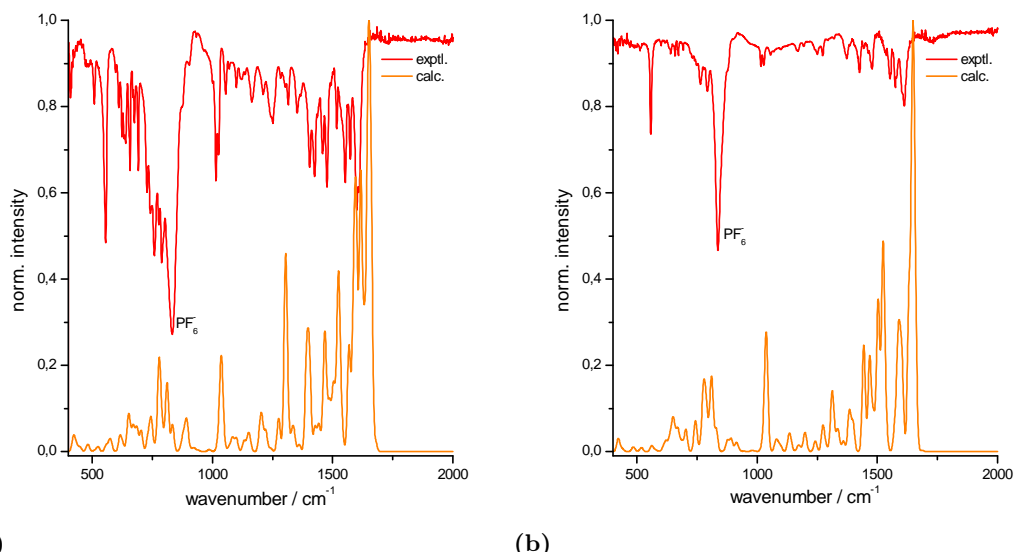


(a)

(b)

Fig. S 41 Overlay (by use of Jmol^[3]) of the experimental determined geometry of $[\text{Zn}(\text{MeATT})_2]^{4+}$ (**2**), color coding by element (a, red) and geometry optimization without any restraints (b, yellow) except that the starting angles of the thiophenyl-linker were adjusted to give the same conformer in minimization).

6.2 Comparison of IR frequency data



(a)

(b)

Fig. S 42 Comparison of measured (red, see also Fig. S 38 and Fig. S 39) and DFT calculated frequencies (orange) in the "fingerprint" region (C–H vibrations omitted for scaling).

6.3 HOMO and LUMO analysis

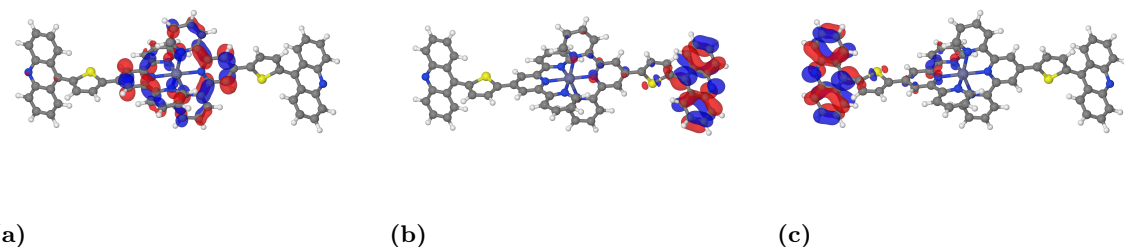


Fig. S 43 LUMO+4 (a, -2.391 eV), LUMO+3 (b, -2.404 eV), and LUMO+2 (c, -2.427 eV ; all close in energy) isoelectron density contours for $[\text{Zn}(\text{ATT})_2]^{2+}$ (**1**) ($0.03\text{ e }a_0^{-3}$, $6\text{ grid points }{\text{\AA}}^{-1}$). Continued in Figure 44 below.

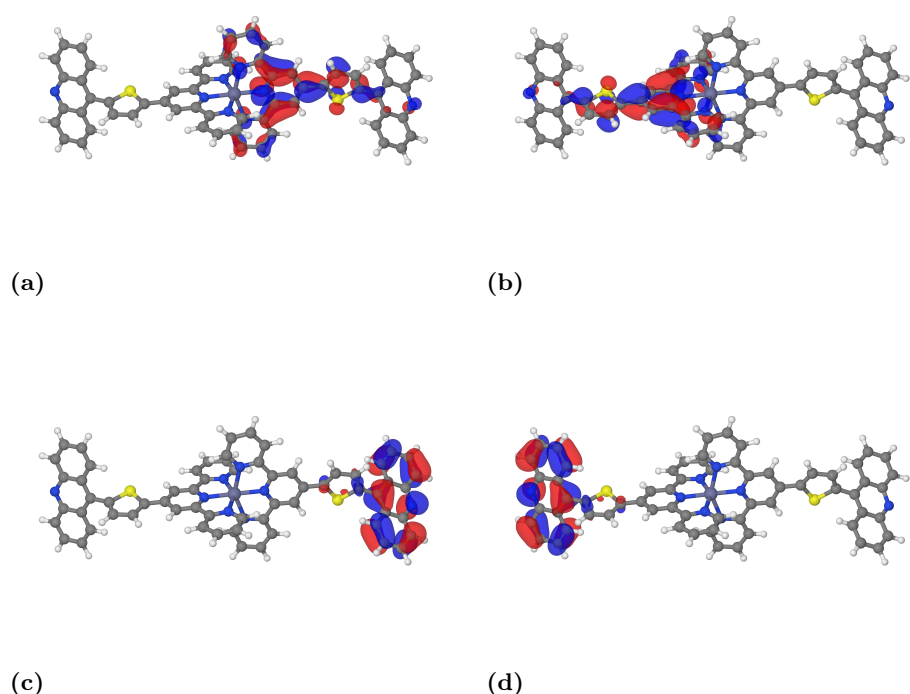


Fig. S 44 Continued frontier orbital plot for $[\text{Zn}(\text{ATT})_2]^{2+}$ (**1**): LUMO (a, -2.815 eV) and LUMO+1 (b, -2.804 eV), and finally HOMO (c, -5.950 eV) and HOMO-1 (d, -5.960 eV ; also all nearly degenerated).

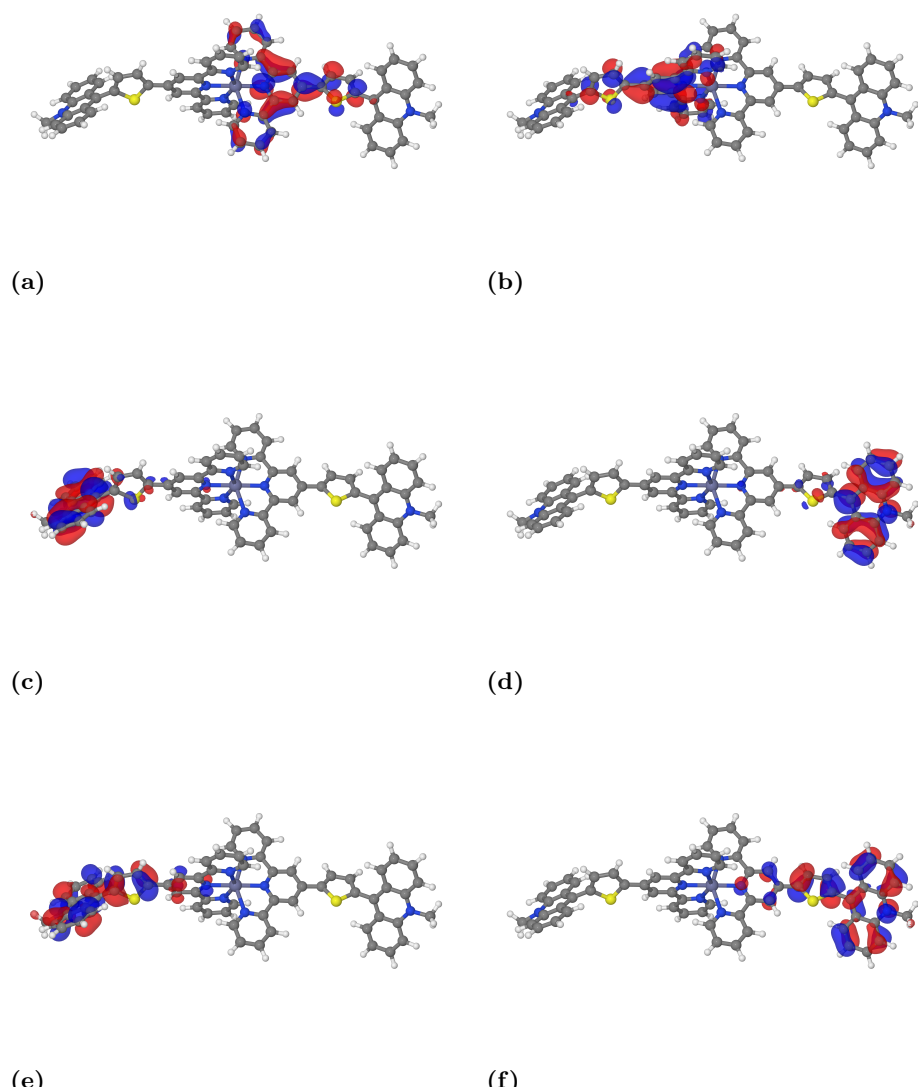


Fig. S 45 LUMO+2 (a, -2.924 eV) and LUMO+3 (b, -2.918 eV nearly isoenergetic), LUMO (c, -3.678 eV) and LUMO+1 (d, -3.676 eV), and HOMO (e, -6.862 eV) and HOMO-1 (f, -6.873 eV) isoelectron density contours for $[Zn(\text{MeATT})_2]^{4+}$ (**2**) ($0.03 e \text{ } a_0^{-3}$, 6 grid points \AA^{-1}).

6.4 Spin density plots

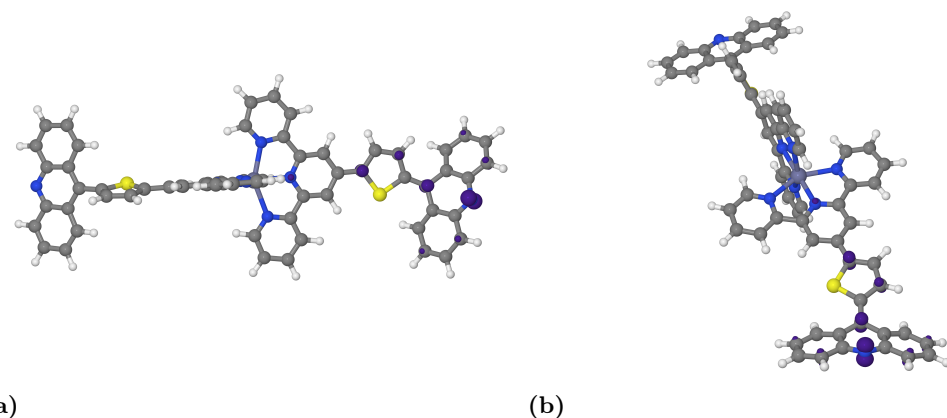


Fig. S 46 Spin density $\Delta(\alpha,\beta)$ (deep violet) for the optimized T_1 state of $[\text{Zn}(\text{ATT})_2][\text{PF}_6]_2$ (**2**) in side (a) and front view (b) as calculated by an unrestricted B3LYP/6-31G(d)/LANL DFT calculation (isocontour value set to $0.02 e a_0^{-3}$; 6 grid points a_0^{-1}).

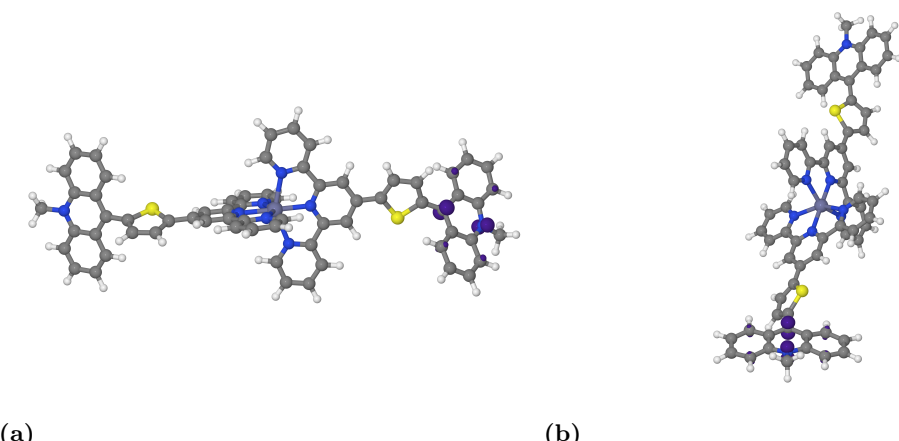


Fig. S 47 Spin density $\Delta(\alpha,\beta)$ (deep violet) for the optimized T_1 state of $[\text{Zn}(\text{MeATT})_2][\text{PF}_6]_4$ (**2**) in side (a) and front view (b) as calculated by an unrestricted B3LYP/6-31G(d)/LANL DFT calculation (isocontour value set to $0.02 e a_0^{-3}$; 6 grid points a_0^{-1}).

6.5 TD-DFT results

#	nm	1000 cm ⁻¹	eV	(f) Assignment; H=HOMO, L=LUMO, L+1=LUMO+1, etc.
1	452.3	22.1	2.74	0.1406 S H-0->L+0 (+98%)
5	395.8	25.3	3.13	0.3710 S H-1->L+2 (+61%) H-1->L+3 (+17%) H-1->L+4 (10%)
6	394.3	25.4	3.14	0.1366 S H-0->L+3 (+52%) H-0->L+4 (+34%)
13	357.6	28.0	3.47	0.8900 S H-3->L+0 (+69%) H-2->L+1 (+19%)
14	353.8	28.3	3.50	0.1121 S H-2->L+1 (+70%) H-3->L+0 (18%)

26	317.9	31.5	3.90	0.1761	S	H-7->L+0 (+23%)	H-6->L+0 (+19%)
	H-3->L+4(14%)		H-3->L+2(10%)	H-3->L+5(+8%)		H-3->L+3(+7%)	
27	317.8	31.5	3.90	0.1350	S	H-6->L+1 (+40%)	H-2->L+2 (+14%)
	H-2->L+5(+13%)		H-2->L+4(+10%)	H-7->L+1(7%)			
63	282.5	35.4	4.39	0.1934	S	H-6->L+2 (+22%)	H-6->L+5 (+18%)
	H-13->L+2(10%)		H-6->L+3(+9%)	H-7->L+2(9%)		H-4->L+5(7%)	
64	281.8	35.5	4.40	0.1163	S	H-0->L+11 (+32%)	H-7->L+5(19%)
	H-0->L+10(+12%)		H-7->L+3(12%)				
65	281.6	35.5	4.40	0.1118	S	H-0->L+11 (+37%)	H-7->L+5 (+16%)
	H-0->L+10(+14%)		H-7->L+3(+11%)				
67	280.5	35.6	4.42	0.1099	S	H-6->L+5 (+29%)	H-7->L+5 (10%)
	H-4->L+3(8%)		H-6->L+4(+8%)	H-4->L+4(7%)		H-9->L+2(7%)	
71	277.5	36.0	4.47	0.1178	S	H-8->L+5 (+18%)	H-8->L+4(17%)
	H-8->L+3(+15%)		H-8->L+2(13%)	H-12->L+3(+9%)		H-3->L+7(6%)	
72	277.2	36.1	4.47	0.1032	S	H-9->L+5 (+23%)	H-9->L+2(+22%)
	H-13->L+2(+22%)		H-9->L+4(+10%)	H-2->L+6(+7%)			
112	252.3	39.6	4.91	0.1553	S	H-15->L+2(+13%)	H-15->L+4(+12%)
	H-15->L+3(11%)		H-14->L+2(10%)	H-14->L+4(10%)		H-14->L+3(+10%)	
	H-14->L+5(+7%)		H-7->L+7(+6%)	H-15->L+5(5%)			
113	252.1	39.7	4.92	0.1114	S	H-2->L+9 (+23%)	H-2->L+8(+14%)
	H-15->L+2(+13%)		H-14->L+2(+13%)	H-14->L+5(+6%)		H-15->L+5(+6%)	
	H-15->L+4(+6%)		H-14->L+4(+5%)				
115	249.9	40.0	4.96	0.4836	S	H-5->L+7(+58%)	H-0->L+12(+24%)
	H-5->L+3(7%)		H-5->L+4(5%)				
116	249.5	40.1	4.97	0.3104	S	H-4->L+6(+73%)	H-1->L+13(+14%)
121	246.0	40.6	5.04	0.1978	S	H-6->L+6(+27%)	H-7->L+6(8%)
	H-1->L+13(8%)		H-15->L+5(+8%)	H-14->L+2(7%)		H-14->L+4(6%)	
	H-14->L+3(+6%)		H-15->L+3(+5%)				
122	245.8	40.7	5.04	0.1714	S	H-14->L+5(+17%)	H-15->L+2(13%)
	H-15->L+5(13%)		H-7->L+7(+13%)	H-14->L+2(+9%)		H-0->L+12(8%)	
	H-5->L+7(+6%)						
123	245.6	40.7	5.05	0.3334	S	H-1->L+13(+22%)	H-14->L+5(+21%)
	H-0->L+12(+11%)		H-5->L+7(9%)	H-4->L+6(9%)			
125	245.4	40.7	5.05	1.3076	S	H-0->L+12(+22%)	H-15->L+5(21%)
	H-5->L+7(18%)		H-1->L+13(10%)				
127	245.1	40.8	5.06	0.3778	S	H-6->L+6(+24%)	H-1->L+13(+14%)
	H-15->L+5(14%)		H-14->L+5(12%)	H-4->L+6(7%)		H-7->L+6(7%)	

Listing 1 Transitions with oscillator strength $f > 0.1$ out of 150 transitions calculated for $[\text{Zn}(\text{ATT})_2]^{2+}$ (**1**).

#	nm	1000 cm ⁻¹	eV	(f)	Assignment; H=HOMO, L=LUMO, L+1=LUMO+1, etc.
1	472.9	21.1	2.62	0.5739	S H-1->L+1(+46%) H-0->L+0(42%)
	H-2->L+1(+6%)				
15	349.6	28.6	3.55	0.6421	S H-0->L+3(+59%) H-1->L+2(36%)
17	336.4	29.7	3.69	0.1664	S H-8->L+0(+68%) H-12->L+0(+15%)
	H-0->L+9(+7%)				
18	335.8	29.8	3.69	0.1700	S H-9->L+1(+67%) H-13->L+1(15%)
	H-1->L+8(7%)				
21	333.0	30.0	3.72	0.1930	S H-4->L+2(+46%) H-5->L+2(19%)
	H-1->L+4(10%)		H-1->L+5(9%)		
22	332.3	30.1	3.73	0.1825	S H-5->L+3(+45%) H-4->L+3(+19%)
	H-0->L+4(13%)		H-0->L+5(+8%)		
25	328.3	30.5	3.78	0.4547	S H-2->L+2(+79%) H-3->L+3(+10%)
26	326.1	30.7	3.80	0.1130	S H-3->L+3(+83%) H-2->L+2(11%)
31	313.5	31.9	3.96	0.1231	S H-0->L+4(+47%) H-5->L+3(+21%)
	H-0->L+5(19%)		H-4->L+3(+6%)		

32	312.9	32.0	3.96	0.1179	S	H-1->L+4 (+44%)	H-1->L+5 (+23%)
	H-4->L+2 (+17%)			H-5->L+2 (9%)			
55	281.0	35.6	4.41	0.7396	S	H-4->L+5 (+69%)	H-5->L+4 (15%)
66	269.2	37.2	4.61	0.2000	S	H-11->L+3 (+42%)	H-11->L+2 (+16%)
	H-10->L+3 (+16%)			H-10->L+2 (10%)			
81	259.8	38.5	4.77	0.1923	S	H-1->L+8 (+73%)	H-2->L+8 (+19%)
82	259.7	38.5	4.77	0.2353	S	H-0->L+9 (+74%)	H-3->L+9 (18%)
90	253.6	39.4	4.89	0.2182	S	H-11->L+4 (+44%)	H-10->L+4 (+14%)
	H-11->L+5 (12%)						
91	253.5	39.5	4.89	0.2283	S	H-10->L+4 (+42%)	H-10->L+5 (+15%)
97	251.1	39.8	4.94	0.1079	S	H-2->L+6 (+38%)	H-2->L+7 (35%)
110	246.1	40.6	5.04	0.3674	S	H-23->L+1 (+32%)	H-2->L+8 (22%)
113	245.2	40.8	5.06	0.5208	S	H-2->L+8 (+36%)	H-23->L+1 (+12%)

Listing 2 Transitions with oscillator strength $f > 0.1$ out of 150 transitions calculated for $[\text{Zn}(\text{MeATT})_2]^{4+}$ (**2**).

6.6 Geometries for $[\text{Zn}(\text{ATT})_2]^{2+}$ (**1**)

The geometries are given in Cartesian coordinates in yxz-file format.^[15]

6.6.1 Optimized S_0 geometry (MeCN)

```
115
ZnATT2_new_calcG631d_FINAL
C      0.04526      1.54019      -2.31115
H     1.11170      1.53897      -2.10787
C     -0.46449      2.13193      -3.46549
H     0.20459      2.60071      -4.17816
C     -1.84228      2.10018      -3.66848
H     -2.28332      2.54792      -4.55316
C     -2.65676      1.48431      -2.71929
H     -3.72873      1.45492      -2.86916
C     -2.07104      0.91247      -1.58618
C     -2.86038      0.23437      -0.51693
C     -4.24892      0.11802      -0.53661
H     -4.81856      0.51666      -1.36618
C     -4.91094      -0.53242      0.52050
C     -4.12103      -1.04786      1.56577
H     -4.59491      -1.53205      2.40830
C     -2.73635      -0.90932      1.51785
C     -1.81555      -1.42713      2.57162
C     -2.26008      -2.14037      3.68878
H     -3.31213      -2.35176      3.83386
C     -1.32896      -2.58723      4.62518
H     -1.65986      -3.14211      5.49711
C     0.02244      -2.31405      4.42544
H     0.77906      -2.64297      5.12876
C     0.38872      -1.60063      3.28566
H     1.42912      -1.36443      3.08424
C     -6.36428      -0.67576      0.54860
C     -7.12191      -1.50916      1.34687
H     -6.69684      -2.19434      2.07112
C     -8.51730      -1.40625      1.11238
H     -9.26211      -1.98706      1.64443
C     -8.84313      -0.48857      0.14024
```

C	-10.18862	-0.12701	-0.36700
C	-10.80996	1.07872	0.02721
C	-10.22315	2.00908	0.94209
H	-9.25326	1.78435	1.37260
C	-10.87663	3.16474	1.28548
H	-10.41806	3.85887	1.98364
C	-12.15887	3.46548	0.73919
H	-12.65721	4.38785	1.02330
C	-12.76171	2.59574	-0.13074
H	-13.74078	2.79663	-0.55468
C	-12.11792	1.37590	-0.51229
C	-12.17775	-0.59294	-1.71934
C	-12.88423	-1.45596	-2.61609
H	-13.86676	-1.13431	-2.94746
C	-12.33170	-2.63753	-3.03461
H	-12.87647	-3.28477	-3.71592
C	-11.03617	-3.02671	-2.58360
H	-10.61016	-3.96387	-2.92983
C	-10.32647	-2.23038	-1.72189
H	-9.34198	-2.53433	-1.38294
C	-10.86847	-0.99207	-1.25324
C	0.10540	-2.84564	-1.08664
H	-0.97162	-2.75988	-0.98016
C	0.67743	-3.94052	-1.73203
H	0.04720	-4.72395	-2.13746
C	2.06557	-3.99209	-1.83635
H	2.55424	-4.82547	-2.33062
C	2.82822	-2.95703	-1.29718
H	3.90774	-2.98873	-1.37462
C	2.18137	-1.89203	-0.66364
C	2.91237	-0.74092	-0.05822
C	4.30059	-0.61923	-0.06040
H	4.91749	-1.39166	-0.50120
C	4.90388	0.50511	0.53142
C	4.05913	1.47196	1.10855
H	4.48552	2.36327	1.54780
C	2.67957	1.28325	1.08797
C	1.70362	2.24593	1.67694
C	2.09054	3.42495	2.32072
H	3.13591	3.68894	2.42083
C	1.11051	4.26872	2.84141
H	1.39630	5.18746	3.34328
C	-0.23095	3.91679	2.70933
H	-1.02458	4.54393	3.09943
C	-0.53797	2.72412	2.05693
H	-1.56812	2.40562	1.93063
C	6.35395	0.67785	0.55588
C	7.09693	1.51589	1.36279
H	6.66192	2.15818	2.11989
C	8.49440	1.43168	1.13363
H	9.23043	2.01024	1.68020
C	8.83607	0.52744	0.15389
C	10.18638	0.19978	-0.36135
C	10.81020	-1.02463	-0.03181
C	10.22343	-2.00685	0.82732
H	9.25126	-1.81064	1.26619

C	10.87990	-3.17742	1.10928
H	10.42078	-3.91051	1.76603
C	12.16583	-3.44275	0.55375
H	12.66639	-4.37776	0.78835
C	12.76983	-2.52282	-0.26198
H	13.75237	-2.69522	-0.69040
C	12.12332	-1.28568	-0.57753
C	12.18540	0.75000	-1.66778
C	12.89659	1.66520	-2.50722
H	13.88348	1.36627	-2.84677
C	12.34294	2.86634	-2.86380
H	12.89119	3.55323	-3.50214
C	11.04099	3.22333	-2.40510
H	10.61292	4.17591	-2.70338
C	10.32691	2.37679	-1.59641
H	9.33696	2.65660	-1.25301
C	10.87048	1.11698	-1.19107
N	-0.73268	0.94655	-1.39668
N	-2.13727	-0.27523	0.49425
N	-0.50179	-1.16866	2.38325
N	-12.76831	0.55797	-1.35667
N	0.83344	-1.84919	-0.56627
N	2.13632	0.19666	0.51101
N	0.39960	1.91049	1.55420
N	12.77730	-0.41804	-1.36769
S	-7.40495	0.25733	-0.51010
S	7.40927	-0.23086	-0.50860
Zn	-0.00039	-0.04113	0.49464

Listing 3 Cartesian coordinates for $[\text{Zn}(\text{ATT})_2]^{2+}$ (**1**) in S_0 state.

6.6.2 Optimized T_1 geometry (MeCN)

115			
ZnATT2_new_calcG631d_FINAL_triplett			
C	-0.07033	0.25010	-2.92732
H	1.00268	0.33201	-2.78352
C	-0.62388	0.22056	-4.20615
H	0.01677	0.27895	-5.07877
C	-2.00814	0.11534	-4.32210
H	-2.48277	0.08918	-5.29764
C	-2.78533	0.04341	-3.16682
H	-3.86194	-0.03792	-3.24839
C	-2.15648	0.07812	-1.91885
C	-2.90230	0.00582	-0.62848
C	-4.28888	-0.10486	-0.54154
H	-4.89033	-0.15790	-1.43987
C	-4.90721	-0.16665	0.72039
C	-4.07752	-0.11309	1.85636
H	-4.51720	-0.13288	2.84376
C	-2.69752	-0.01329	1.69976
C	-1.73754	0.04417	2.84074
C	-2.13830	-0.01679	4.17876
H	-3.18350	-0.11210	4.44541
C	-1.17169	0.04525	5.18147
H	-1.46816	-0.00032	6.22440
C	0.17036	0.16492	4.82727

H	0.95337	0.21621	5.57537
C	0.49187	0.21705	3.47217
H	1.52309	0.30856	3.14496
C	-6.35609	-0.28427	0.86541
C	-7.07122	-0.65185	1.98753
H	-6.60981	-0.91951	2.93110
C	-8.47502	-0.67629	1.78355
H	-9.19079	-0.94538	2.55195
C	-8.84963	-0.31985	0.50848
C	-10.21762	-0.24397	-0.05835
C	-10.85330	1.00286	-0.24917
C	-10.25901	2.25580	0.10270
H	-9.27113	2.26306	0.55058
C	-10.92716	3.43465	-0.10789
H	-10.46248	4.37684	0.16761
C	-12.23247	3.43866	-0.68157
H	-12.74234	4.38434	-0.84151
C	-12.84265	2.26018	-1.02152
H	-13.83892	2.23498	-1.45211
C	-12.18388	1.00667	-0.81455
C	-12.23694	-1.29833	-0.96038
C	-12.95117	-2.48426	-1.32324
H	-13.95046	-2.36045	-1.72905
C	-12.38543	-3.72147	-1.16237
H	-12.93637	-4.61497	-1.44165
C	-11.06817	-3.84783	-0.63130
H	-10.63205	-4.83579	-0.51588
C	-10.35028	-2.73728	-0.26849
H	-9.34915	-2.84235	0.13542
C	-10.90514	-1.42644	-0.41191
C	0.04625	-2.99879	0.24788
H	-1.02578	-2.85500	0.34217
C	0.59581	-4.27741	0.18239
H	-0.04642	-5.14978	0.22519
C	1.97921	-4.39358	0.06166
H	2.45120	-5.36927	0.00692
C	2.75818	-3.23893	0.01100
H	3.83369	-3.32077	-0.08350
C	2.13375	-1.98978	0.08290
C	2.88263	-0.70004	0.03508
C	4.26535	-0.61652	-0.07799
H	4.86287	-1.51745	-0.12844
C	4.89606	0.64936	-0.11925
C	4.05938	1.78841	-0.04246
H	4.49308	2.77764	-0.08123
C	2.68437	1.63170	0.07291
C	1.72793	2.77305	0.16187
C	2.13123	4.11211	0.13553
H	3.17701	4.37850	0.04624
C	1.16822	5.11528	0.22638
H	1.46774	6.15822	0.20730
C	-0.17505	4.76217	0.34145
H	-0.95566	5.51093	0.41495
C	-0.49963	3.40758	0.36020
H	-1.53152	3.08137	0.44806
C	6.32570	0.78664	-0.23671

C	7.08969	1.96441	-0.17942
H	6.65930	2.94135	0.00598
C	8.44938	1.76953	-0.33163
H	9.16808	2.57162	-0.24392
C	8.84239	0.40757	-0.52315
C	10.13971	-0.10382	-0.62046
C	10.47881	-1.52970	-0.47620
C	9.69410	-2.59608	-0.92170
H	8.81992	-2.41045	-1.53538
C	10.03693	-3.92793	-0.63518
H	9.40235	-4.72981	-0.99962
C	11.18006	-4.21576	0.11188
H	11.43532	-5.24355	0.35124
C	12.00774	-3.17563	0.52616
H	12.92322	-3.36774	1.07688
C	11.70662	-1.83120	0.20864
C	12.49229	0.36089	0.01441
C	13.59470	1.24176	0.11009
H	14.46296	0.90332	0.66683
C	13.58011	2.48012	-0.52619
H	14.44103	3.13796	-0.45684
C	12.46465	2.85527	-1.27823
H	12.45632	3.79946	-1.81399
C	11.34227	2.01400	-1.34763
H	10.49912	2.31193	-1.96153
C	11.30841	0.79294	-0.67025
N	-0.81246	0.18076	-1.81476
N	-2.14016	0.04703	0.47727
N	-0.43295	0.15883	2.50522
N	-12.84174	-0.11444	-1.15438
N	0.79053	-1.88588	0.19971
N	2.11943	0.40733	0.11012
N	0.42214	2.43908	0.27295
N	12.64286	-0.89169	0.53785
S	-7.44780	0.04279	-0.46705
S	7.37553	-0.60465	-0.47320
Zn	-0.00315	0.22341	0.29057

Listing 4 Cartesian coordinates for $[\text{Zn}(\text{ATT})_2]^{2+}$ (**1**) in T_1 state.

6.7 Geometries for $[\text{Zn}(\text{MeATT})_2]^{4+}$ (2)

6.7.1 Optimized S_0 geometry (MeCN)

```
123
ZnMeATT_calcG631d_FINAL-3rdtight-freq
C      -0.10932      -2.29313      1.35754
H      -1.17098      -2.06662      1.36592
C       0.37399      -3.48495      1.89502
H      -0.31159      -4.20349      2.32972
C       1.74689      -3.71663      1.85554
H       2.16763      -4.63017      2.26297
C       2.58314      -2.75780      1.28518
H       3.65194      -2.92828      1.25233
C       2.02316      -1.58743      0.76548
C       2.83744      -0.50550      0.13969
C       4.22429      -0.55950      0.00474
H       4.77313      -1.42941      0.34185
C       4.90707      0.51504      -0.59035
C       4.14715      1.61156      -1.03549
H       4.64291      2.46548      -1.47591
C       2.76233      1.59627      -0.88312
C       1.86805      2.70549      -1.32516
C       2.34260      3.86554      -1.94387
H       3.39965      4.00649      -2.13149
C       1.43499      4.85302      -2.32463
H       1.78914      5.75889      -2.80581
C       0.07725      4.66022      -2.08025
H      -0.66181      5.40229      -2.36020
C      -0.31922      3.47688      -1.45965
H      -1.36588      3.28030      -1.24846
C       6.36197      0.51285      -0.75025
C       7.12427      1.29872      -1.58992
H       6.70446      2.02007      -2.28085
C       8.51680      1.05390      -1.48479
H       9.26641      1.57239      -2.07132
C       8.82627      0.06898      -0.57404
C      10.17332      -0.41652      -0.20095
C      11.03564      0.41895      0.54500
C      10.62241      1.70284      1.01573
H       9.62127      2.04062      0.78028
C      11.46134      2.48928      1.76118
H      11.13180      3.45970      2.11639
C      12.75565      2.01839      2.08730
H      13.41037      2.62826      2.70156
C      13.19989      0.78753      1.65758
H      14.18021      0.45272      1.96426
C      12.36029      -0.03897      0.86816
C      11.92796      -2.14415      -0.20909
C      12.32476      -3.47043      -0.51880
H      13.28194      -3.85380      -0.19590
C      11.47250      -4.30676      -1.20483
H      11.79219      -5.32104      -1.42165
C      10.19638      -3.86742      -1.63202
H      9.55489      -4.53363      -2.19863
C      9.77561      -2.60182      -1.31731
```

H	8.80089	-2.25756	-1.63802
C	10.60481	-1.71046	-0.56958
C	14.19741	-1.66029	0.61798
H	14.82149	-0.77233	0.57225
H	14.50366	-2.31248	-0.19463
H	14.32968	-2.16549	1.57803
C	-0.13488	-0.82756	-2.96584
H	0.94289	-0.72606	-2.88420
C	-0.71692	-1.41409	-4.08836
H	-0.09366	-1.77767	-4.89746
C	-2.10533	-1.51549	-4.13347
H	-2.60146	-1.96549	-4.98722
C	-2.85878	-1.03095	-3.06500
H	-3.93854	-1.10697	-3.09149
C	-2.20232	-0.45412	-1.97422
C	-2.92297	0.09169	-0.78754
C	-4.31110	0.08847	-0.65429
H	-4.93727	-0.30502	-1.44457
C	-4.89848	0.62084	0.50592
C	-4.04708	1.14467	1.49489
H	-4.46578	1.53606	2.41178
C	-2.66854	1.13215	1.29197
C	-1.68211	1.67340	2.27157
C	-2.05729	2.26958	3.47885
H	-3.10007	2.36508	3.75439
C	-1.06826	2.74997	4.33615
H	-1.34465	3.21497	5.27686
C	0.26962	2.62594	3.96869
H	1.06993	2.98586	4.60528
C	0.56467	2.02242	2.74743
H	1.59190	1.90552	2.41637
C	-6.34964	0.64171	0.69590
C	-7.08028	1.43675	1.55493
H	-6.63833	2.19222	2.19374
C	-8.47587	1.19393	1.50027
H	-9.20509	1.73131	2.09545
C	-8.82136	0.22004	0.58984
C	-10.17363	-0.29563	0.28771
C	-10.78137	-0.03414	-0.96178
C	-10.16859	0.80995	-1.93768
H	-9.21471	1.26502	-1.70389
C	-10.78083	1.07134	-3.13581
H	-10.30722	1.72169	-3.86321
C	-12.04996	0.50841	-3.41038
H	-12.54648	0.73430	-4.34863
C	-12.68564	-0.30417	-2.49794
H	-13.67349	-0.67470	-2.73068
C	-12.06979	-0.60077	-1.25548
C	-12.18186	-1.56092	0.94468
C	-12.91524	-2.23923	1.95134
H	-13.92344	-2.58163	1.76785
C	-12.36487	-2.43293	3.19885
H	-12.94871	-2.94348	3.95806
C	-11.05874	-1.98118	3.50437
H	-10.63534	-2.16880	4.48516
C	-10.33901	-1.29864	2.55868

H	-9.34301	-0.94036	2.78425
C	-10.88130	-1.03485	1.26346
C	-13.92771	-2.12015	-0.70151
H	-14.80747	-1.50465	-0.49745
H	-13.98493	-3.05175	-0.14597
H	-13.88518	-2.37477	-1.75685
N	0.68930	-1.36942	0.80747
N	2.14149	0.55448	-0.30313
N	0.54845	2.52533	-1.09135
N	12.78269	-1.27128	0.42433
N	-0.85383	-0.36021	-1.93703
N	-2.13908	0.60889	0.17265
N	-0.38135	1.55858	1.92072
N	-12.68953	-1.40267	-0.32449
S	7.38453	-0.55981	0.18235
S	-7.40687	-0.42116	-0.20748
Zn	-0.00008	0.58751	-0.07839

Listing 5 Cartesian coordinates for $[\text{Zn}(\text{MeATT})_2]^{4+}$ (**2**) in S_0 state.

6.7.2 Optimized T_1 geometry (MeCN)

123			
ZnMeATT_calcG631d_FINAL_triplett.			
C	0.03304	0.80919	-2.66863
H	1.10019	0.86457	-2.47727
C	-0.48011	1.04118	-3.94373
H	0.18714	1.28055	-4.76395
C	-1.85873	0.95740	-4.12435
H	-2.30247	1.13180	-5.09912
C	-2.67083	0.64623	-3.03450
H	-3.74376	0.58189	-3.16508
C	-2.08148	0.42473	-1.78674
C	-2.86840	0.08872	-0.56478
C	-4.25523	-0.05722	-0.55247
H	-4.82604	0.04718	-1.46615
C	-4.90932	-0.36626	0.65200
C	-4.12449	-0.52124	1.80824
H	-4.60136	-0.72975	2.75622
C	-2.74068	-0.37942	1.72343
C	-1.81865	-0.53680	2.88536
C	-2.26213	-0.86238	4.17023
H	-3.31403	-1.01673	4.37558
C	-1.32991	-0.99107	5.19895
H	-1.65962	-1.24297	6.20166
C	0.02080	-0.79380	4.92163
H	0.77851	-0.88446	5.69167
C	0.38575	-0.47412	3.61495
H	1.42589	-0.31256	3.34946
C	-6.36239	-0.53065	0.72234
C	-7.08952	-1.23080	1.66258
H	-6.63860	-1.76941	2.48785
C	-8.48690	-1.21584	1.42127
H	-9.21321	-1.71760	2.05016
C	-8.83657	-0.48598	0.30748
C	-10.19703	-0.27481	-0.23449
C	-10.81133	0.99640	-0.17887

C	-10.16185	2.12842	0.40251
H	-9.18336	1.99469	0.84526
C	-10.75733	3.36267	0.40995
H	-10.25079	4.21308	0.85339
C	-12.03649	3.52585	-0.17398
H	-12.49314	4.51002	-0.20204
C	-12.72114	2.45654	-0.70715
H	-13.68715	2.62941	-1.15922
C	-12.14284	1.16126	-0.69664
C	-12.22826	-1.16115	-1.31100
C	-12.89523	-2.24126	-1.94326
H	-13.88285	-2.11624	-2.36292
C	-12.26996	-3.46153	-2.07371
H	-12.79434	-4.26997	-2.57312
C	-10.95659	-3.67181	-1.58990
H	-10.48258	-4.63987	-1.71073
C	-10.28261	-2.64028	-0.99015
H	-9.26894	-2.78078	-0.63740
C	-10.88726	-1.35608	-0.82859
C	-14.26343	0.21283	-1.51407
H	-14.71020	0.96918	-0.87510
H	-14.77670	-0.72325	-1.31373
H	-14.37964	0.48948	-2.56498
C	0.09846	-3.00342	-0.17611
H	-0.97887	-2.88637	-0.11029
C	0.66981	-4.24355	-0.45609
H	0.03872	-5.11116	-0.61179
C	2.05836	-4.32790	-0.52829
H	2.54645	-5.27270	-0.74436
C	2.82225	-3.18033	-0.31985
H	3.90216	-3.23674	-0.37629
C	2.17611	-1.97232	-0.04265
C	2.90820	-0.69405	0.19293
C	4.29701	-0.58183	0.16909
H	4.91357	-1.45337	-0.00889
C	4.89886	0.66879	0.40088
C	4.05438	1.76815	0.64753
H	4.48057	2.74968	0.80163
C	2.67388	1.58465	0.66783
C	1.69601	2.68220	0.92282
C	2.08123	3.99991	1.18574
H	3.12646	4.28058	1.21975
C	1.09900	4.96387	1.40875
H	1.38351	5.99091	1.61337
C	-0.24256	4.59135	1.36519
H	-1.03757	5.30925	1.53211
C	-0.54788	3.25757	1.10014
H	-1.57822	2.91830	1.05724
C	6.34791	0.83877	0.38931
C	7.08481	1.88895	0.91611
H	6.64076	2.72368	1.44542
C	8.47451	1.74518	0.74788
H	9.19693	2.44743	1.14625
C	8.84772	0.57432	0.09345
C	10.17342	0.12336	-0.27680
C	10.63660	-1.21347	0.04582

C	9.94707	-2.06553	0.91925
H	9.02749	-1.72503	1.37677
C	10.42311	-3.34837	1.24370
H	9.84291	-3.97485	1.91313
C	11.62911	-3.79669	0.72375
H	12.01733	-4.77722	0.97544
C	12.36346	-2.96147	-0.12388
H	13.32502	-3.30423	-0.48118
C	11.88519	-1.68386	-0.47021
C	12.37270	0.51218	-1.38902
C	13.32138	1.38150	-1.96120
H	14.30151	1.01683	-2.23833
C	13.02602	2.73246	-2.16558
H	13.77504	3.38516	-2.59939
C	11.76563	3.20813	-1.83209
H	11.49818	4.24297	-2.01895
C	10.81667	2.35085	-1.24465
H	9.83030	2.74097	-1.03184
C	11.10492	1.01331	-0.94367
C	13.77637	-1.41971	-2.05003
H	14.69872	-1.38960	-1.46222
H	13.90401	-0.85614	-2.97081
H	13.54074	-2.44666	-2.31867
N	-0.74248	0.50956	-1.61873
N	-2.14697	-0.07662	0.55612
N	-0.50560	-0.34838	2.62331
N	-12.83178	0.06740	-1.16833
N	0.82762	-1.89819	0.02557
N	2.13241	0.37446	0.44234
N	0.39167	2.32756	0.88509
N	12.65133	-0.84983	-1.28547
S	-7.42452	0.18060	-0.47300
S	7.40747	-0.35071	-0.32987
Zn	-0.00650	0.14629	0.48048

Listing 6 Cartesian coordinates for $[\text{Zn}(\text{MeATT})_2]^{4+}$ (**2**) in T_1 state.

References and Notes

- [1] G. R. Fulmer, A. J. M. Miller, N. H. Sherden, H. E. Gottlieb, A. Nudelman, B. M. Stoltz, J. E. Bercaw and K. I. Goldberg, NMR Chemical Shifts of Trace Impurities: Common Laboratory Solvents, Organics, and Gases in Deuterated Solvents Relevant to the Organometallic Chemist, *Organometallics*, 2010, **29**, 2176–2179, DOI: 10.1021/om100106e.
- [2] J. Eberhard, K. Peuntinger, R. Fröhlich, D. M. Guldi and J. Mattay, *to be published/in preparation*.
- [3] *Jmol: an open-source Java viewer for chemical structures in 3D*, <http://www.jmol.org/>.
- [4] S. I. Gorelsky, *SWizard program*, 2010, <http://www.sg-chem.net/>.
- [5] S. Leonid, *Chemissian*, 2012, <http://www.chemissian.com/>.
- [6] A. G. Griesbeck and M. Cho, 9-Mesityl-10-methylacridinium: An Efficient Type II and Electron-Transfer Photooxygenation Catalyst, *Org. Lett.*, 2007, **9**, 611–613, DOI: 10.1021/o10628661.
- [7] P. Schieberle, W. Maier, J. Firl and W. Grosch, HRGC separation of hydroperoxides formed during the photosensitized oxidation of (R)-(+)-Limonene, *J. High Resol. Chromatogr.*, 1987, **10**, 588–593, DOI: 10.1002/jhrc.1240101102.
- [8] (a) C. S. Foote, S. Wexler and W. Ando, Chemistry of singlet oxygen III. Product selectivity, *Tetrahedron Letters*, 1965, **6**, 4111–4118, DOI: 10.1016/S0040-4039(01)99574-7; (b) C. S. Foote, Photosensitized oxygenations and the role of singlet oxygen, *Acc. Chem. Res.*, 1968, **1**, 104–110, DOI: 10.1021/ar50004a002.
- [9] (a) G. O. Schenck, K. Gollnick, G. Buchwald, S. Schroeter and G. Ohloff, Zur chemischen und sterischen Selektivität der photosensibilisierten O₂-Übertragung auf (+)-Limonen und (+)-Carvomenthen, *Justus Liebigs Ann. Chem.*, 1964, **674**, 93–117, DOI: 10.1002/jlac.19646740111; (b) K. Gollnick and G. O. Schenck, Mechanism and stereoselectivity of photosensitized oxygen transfer reactions, *Pure Appl. Chem.*, 1964, **9**, 507–526, DOI: 10.1351/pac196409040507; (c) K. Gollnick and A. Schnatterer, 9,10-Dicyanoanthracene-sensitized photooxygenation of α,α' -dimethylstilbenes. Mechanism and kinetics of the competing singlet oxygen and electron transfer photooxygenation reactions, *Photochem Photobiol*, 1986, **43**, 365–378, DOI: 10.1111/j.1751-1097.1986.tb05617.x.
- [10] T. Sato and E. Murayama, The Unsensitized Photooxidation of (+)-Limonene, 1,2-Dimethylcyclohexene, and *endo*-Dicyclopentadiene, *Bull. Chem. Soc. Jpn.*, 1974, **47**, 715–719, DOI: 10.1246/bcsj.47.715.
- [11] B. C. Clark, B. B. Jones and G. A. Iacobucci, Characterization of the hydroperoxides derived from singlet oxygen oxidation of (+)-limonene, *Tetrahedron*, 1981, **37**, 405–409, DOI: 10.1016/0040-4020(81)85078-8.

- [12] M. Montalti, A. Credi, L. Prodi and T. M. Gandolfi, *Handbook of photochemistry*, CRC/Taylor & Francis, Boca Raton, 3rd edn., 2006.
- [13] D. Wöhrle, W.-D. Stohrer and M. W. Tausch, *Photochemie*, Wiley-VCH, Weinheim, 2005.
- [14] S. L. Murov, I. Carmichael and G. L. Hug, *Handbook of photochemistry*, Marcel Dekker, 2nd edn., 1993.
- [15] (a) As specified by OpenBabel see <http://openbabel.sourceforge.net/wiki/XYZ>; (b) *OpenBabel v2.3.0*, <http://openbabel.org>; (c) N. M. O'Boyle, M. Banck, C. A. James, C. Morley, T. Vandermeersch and G. R. Hutchison, Open Babel: An open chemical toolbox, *J. Cheminf.*, 2011, **3**, 33, DOI: 10.1186/1758-2946-3-33; (d) R. Guha, M. T. Howard, G. R. Hutchison, P. Murray-Rust, H. Rzepa, C. Steinbeck, J. Wegner and E. L. Willighagen, The Blue Obelisk: Interoperability in Chemical Informatics, *J. Chem. Inf. Model.*, 2006, **46**, 991–998, DOI: 10.1021/ci050400b.